DEMONSTRATION REPORT

Practical UXO Classification: Enhanced Data Processing Strategies for Technology Transition – Fort Ord

Dynamic and Cued MetalMapper Processing and Classification

ESTCP Project MR-201421

MAY 2017

Kevin Kingdon
Black Tusk Geophysics

Page Intentionally Left Blank

Page Intentionally Left Blank

REPORT DOCUMENTATION PAGE

Form Approved
OMB No. 0704-0188

1. REPORT DATE *(DD-MM-YYYY)*	**2. REPORT TYPE**	**3. DATES COVERED** *(From - To)*
06-06-2017	Demonstration Report	

4. TITLE AND SUBTITLE

Practical UXO Classification: Enhanced Data Processing Strategies for Technology Transition

5a. CONTRACT NUMBER

5b. GRANT NUMBER

5c. PROGRAM ELEMENT NUMBER

6. AUTHOR(S)

Kevin Kingdon

5d. PROJECT NUMBER

5e. TASK NUMBER

5f. WORK UNIT NUMBER

7. PERFORMING ORGANIZATION NAME(S) AND ADDRESS(ES)

Black Tusk Geophysics
401 / 1755 West Broadway
Vancouver, BC V6J 4S5

8. PERFORMING ORGANIZATION REPORT NUMBER

9. SPONSORING / MONITORING AGENCY NAME(S) AND ADDRESS(ES)

Environmental Scientific Technology Certification Program
4800 Mark Center, Suite 17D03
Alexandria, VA 22350

10. SPONSOR/MONITOR'S ACRONYM(S)

ESTCP

11. SPONSOR/MONITOR'S REPORT NUMBER(S)

MR-201433

12. DISTRIBUTION / AVAILABILITY STATEMENT

Unlimited

13. SUPPLEMENTARY NOTES

14. ABSTRACT

The objective of this project is to demonstrate advanced methods for the detection and classification of unexploded ordnance (UXO) in a production setting. At the Fort Ord demonstration, the specific classification objectives were:

1. Demonstrate if large munitions, such as 155mm projectiles to a depth of 2 feet, can be confidently classified within the range of background conditions (medium to high metallic density) that exist in the Impact Area at Fort Ord.

2. Demonstrate if smaller munitions such as 40mm projectiles can be confidently classified within the range of background conditions at Fort Ord.

3. Classify all TOI.

15. SUBJECT TERMS

Base Realignment and Closure, Comma Separated Variable, Digital Geophysical Mapping, Electromagnetic Induction, Instrument Verification Strip, Time Domain Electromagnetic, Unexploded Ordnance

16. SECURITY CLASSIFICATION OF:			**17. LIMITATION OF ABSTRACT**	**18. NUMBER OF PAGES**	**19a. NAME OF RESPONSIBLE PERSON**
a. REPORT	**b. ABSTRACT**	**c. THIS PAGE**			Kevin Kingdon
Demonstration Report				53	**19b. TELEPHONE NUMBER** *(include area code)* 604-441-6491

Standard Form 298 (Rev. 8-98)
Prescribed by ANSI Std. Z39.18

Page Intentionally Left Blank

DEMONSTRATION REPORT

Project: MR-201421

TABLE OF CONTENTS

Page

LIST OF FIGURES

Page

LIST OF FIGURES

Page

LIST OF TABLES

Page

ACRONYMS AND ABBREVIATIONS

BRAC	Base Realignment and Closure
BTG	Black Tusk Geophysics
CA	California
cm	Centimeter
CSV	Comma Separated Variable
DGM	Digital Geophysical Mapping
EM	Electromagnetic
EMI	Electromagnetic Induction
ESTCP	Environmental Security Technology Certification Program
IVS	Instrument Verification Strip
m	Meter
mm	Millimeter
ms	Millisecond
MEC	Munitions and Explosives of Concern
MR	Munitions Response
QA	Quality Assurance
QC	Quality Control
ROC	Receiver Operating Characteristic
RTK	Real-time Kinematic
s	Second
SNR	Signal to Noise Ratio
SOI	Single Object Inversion
2OI	Two Object Inversion
3OI	Three Object Inversion
TOI	Target of Interest
TDEM	Time Domain Electromagnetic
UBC-GIF	University of British Columbia Geophysical Inversion Facility
USACE	United States Army Corps of Engineers
UXO	Unexploded Ordnance

Page Intentionally Left Blank

EXECUTIVE SUMMARY

This report describes processing of dynamic and cued MetalMapper data collected as part of the Environmental Science Technology Certification Program (ESTCP) demonstration conducted in 2015 at the former Fort Ord, CA. The data was processed under project ESTCP MR- 201421 "Practical UXO Classification: Enhanced Data Processing Strategies for Technology Transition." The objective of this project is to demonstrate advanced methods for the detection and classification of unexploded ordnance (UXO) in a production setting. At the Fort Ord demonstration, the specific classification objectives were:

1. Demonstrate if large munitions, such as 155mm projectiles to a depth of 2 feet, can be confidently classified within the range of background conditions (medium to high metallic density) that exist in the Impact Area at Fort Ord.

2. Demonstrate if smaller munitions such as 40mm projectiles can be confidently classified within the range of background conditions at Fort Ord.

3. Classify all TOI.

A detailed evaluation of the performance objectives outlined in the demonstration plan is provided in a companion report under ESTCP project MR-201420. Here we present the following key results from the processing of dynamic and cued data:

1. Target picking at a late time channel (e.g. 9.2 ms) in the dynamic MetalMapper data significantly reduces the amount of clutter detected. Large, slow decaying targets that are underneath clutter and are undetectable in EM61 data can be resolved at late times in the MetalMapper detection data. We recommend that long off-time dynamic MetalMapper data is used for detection of large TOI in follow-on work at Fort Ord.

2. The primary objective of confident classification of large munitions such as 155mm projectiles was achieved using the MetalMapper cued data acquired in low, medium and high density grids at Fort Ord.

3. Although, there were 11 small TOI missed in our cued MetalMapper diglist, the classification results indicate that 95% of smaller munitions can be confidently classified within the range of background conditions at Fort Ord.

Page Intentionally Left Blank

1.0 INTRODUCTION

The former Fort Ord, located in Monterey County, California, is a closed installation that has an ongoing munitions response program managed by the U.S. Corps of Engineers (USACE) Sacramento District on behalf of the Fort Ord Base Realignment and Closure (BRAC) Office. In 2014, ESTCP conducted a demonstration of advanced classification technology at Fort Ord. The objectives of this project were to demonstrate the ability to collect data in dynamic and cued modes for munitions and explosives of concern (MEC) detection and identification using the MetalMapper, while simultaneously transferring the technology from the researchers to production companies and to gain regulator acceptance.

The subject area was within Units 11 and 12 in the Impact Area MRA at the former Fort Ord. Units 11 and 12 cover approximately 476 acres. The complete area had full coverage surface MEC remediation, plus digital geophysical mapping (DGM) was performed using a vehicle towed array of three Time-domain Electromagnetic (TDEM) metal detectors (EM61-MK2) over the complete site except small areas where terrain and a stand of oak trees precluded data collection (Figure 1)

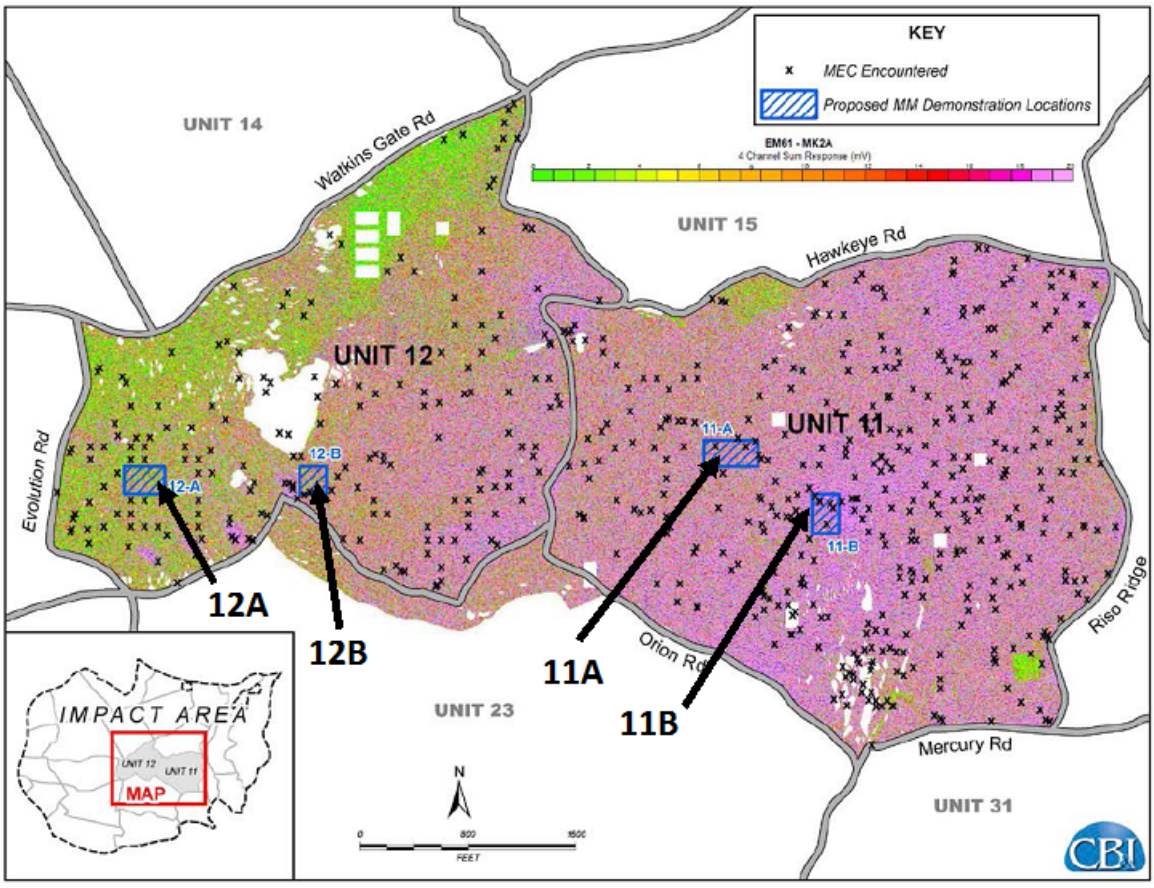

Figure 1. Units 11 and 12 of the Ft. Ord Impact Area.

Gridded image shows EM-61 detection map. MetalMapper grids surveyed under this demonstration project are identified by blue polygons.

Surface sweeps identified MEC items throughout Units 11 and 12, including 37mm, 40mm, 57mm, 60mm, 75mm, 90mm, 105mm, and 155mm projectiles. The results of the DGM following surface removal showed very high EM61-MK2 anomaly densities throughout most of the two Units. The results of the DGM indicated that a variety of MEC items may be present in the subsurface. The BRAC Office was particularly interested in determining if advanced classification methods could be used to locate large MEC items such as 155mm projectiles, as well as sensitive munitions such as 40mm projectiles.

Given that there was a wide variety of possible munitions and that the area was considered to have very high anomaly density, a primary goal was to demonstrate if large munitions such as 155mm projectiles at depths to 2 feet could be confidently classified within a challenging high metallic debris background. In order to determine if this was possible, four representative grids of high, medium, and low anomaly densities (Figure 1) were surveyed with the MetalMapper in both dynamic and cued modes for detection and classification, respectively.

In the remainder of this report we provide a brief description of the hardware and data processing technologies that were used for this demonstration. We discuss detection of TOI using dynamic MetalMapper data, and then in section **4.0** turn to classification with cued MetalMapper data. We provide a summary of our classification approach and a retrospective analysis for small TOI that were missed in our classification diglist. We conclude with lessons learned and recommendations for future work.

2.0 TECHNOLOGY DESCRIPTION

2.1 DETECTION

The MetalMapper is an advanced time-domain electromagnetic (TDEM) sensor designed specifically for classification of MEC. The antenna platform includes three mutually orthogonal transmitter loops and a spatial array of seven 3-axis receiver antennas providing 21 independent measurements of the transient secondary magnetic field.

Figure 2. Dynamic MetalMapper survey at Ft. Ord.

Advanced TDEM sensors such as the MetalMapper acquire detection data for digital geophysical mapping (DGM) with a higher resolution and longer off-times than conventional EM-61 arrays (Figure 3). These features are particularly advantageous at a highly cluttered site such as Fort Ord where the primary target of interest is a large, slow decaying munition.

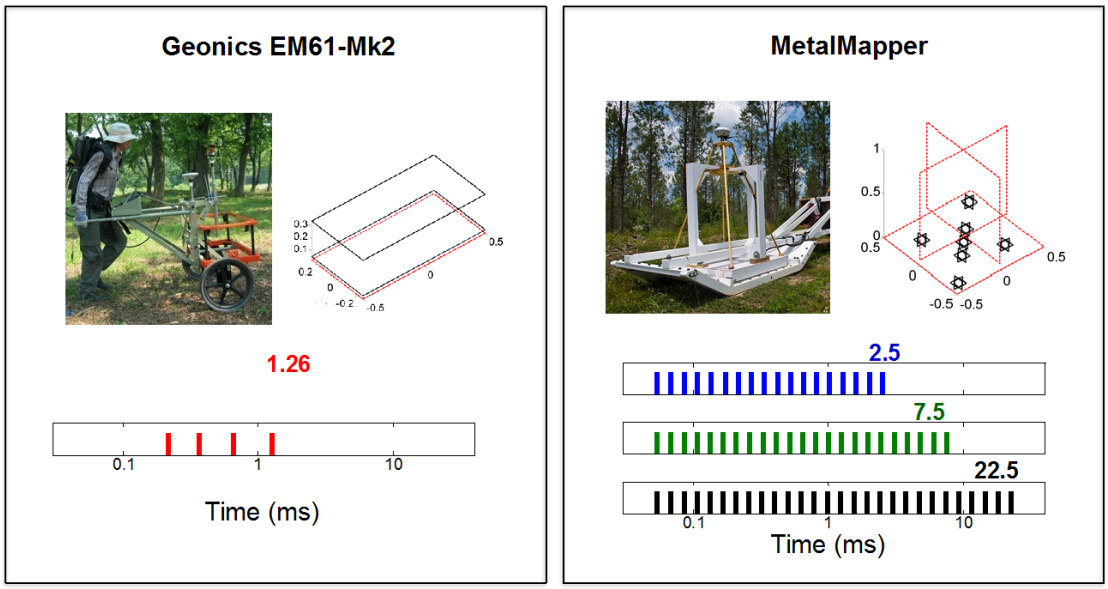

Figure 3. Comparison of EM61 (left) and MetalMapper (right) Sensors.

Within each panel we show an image of the sensor (top left), sensor geometry (top right, transmitters in red, receivers in black) and measurement off-times (bottom). For the MetalMapper, three possible off-times are shown, extending as late as 22.5 ms.

2.2 CLASSIFICATION

Target classification is usually carried out using cued interrogation data acquired over anomalies initially identified in the detection data. These cued interrogations eliminate relative positional errors by acquiring data with a stationary sensor. The multi-static, multi-component geometry of advanced sensors such as the MetalMapper allows for reliable target characterization with a single cued sounding. In-field inversions of cued soundings help to ensure that the sensor is optimally positioned over each target.

Cued interrogation data are inverted using a dipole model to recover estimates of extrinsic (location, depth, and orientation) and intrinsic (dipole polarizabilities) parameters for each interrogated target. The estimated polarizabilities for each recovered dipole source are then matched against a pre-defined library to identify likely targets of interest (TOI) at the site. For this demonstration, all classification processing was carried out using the *UXOLab* software package developed jointly by BTG and UBC-GIF.

3.0 DETECTION WITH THE METALMAPPER AT FORT ORD

For this demonstration we investigated whether dynamic MetalMapper measurements could identify responses from large TOI at late times, after small metallic surface debris has decayed away.

Extending the dynamic MetalMapper off-time window out to approximately 25 ms while maintaining an along-track sampling rate of 0.1s necessarily reduced the number of stacks for each dynamic sounding. This reduced the signal to noise ratio (SNR) of the dynamic data. To ensure that noise levels did not preclude detection of large TOI, we collected dynamic MetalMapper data at the testpit over a range of items. We found that we could both detect and recover high quality polarizabilities for a range of TOI using dynamic testpit data. In order to ensure that these testpit findings held for the high metallic debris grids at the site, we also went out into the high density 11-B grid and collected a swath of dynamic data with each of the short, medium and long time windows. A quality control (QC) seed was detected in the surveyed swath, and our measurements confirmed that both detection and recovery of high quality polarizabilities were feasible with a long off-time in this survey environment.

Figure 4 compares the unfiltered data for the latest time channel (1.26 ms) of EM61 data acquired at Fort Ord grid 11-B with a comparable time channel (1.23 ms) of dynamic MetalMapper data. Large, distinct anomalies are present in both data sets and correlate well with each other. As expected, the dynamic MetalMapper does a better job of resolving individual targets in the dense region in the northeast corner of the grid. MetalMapper dynamic data are more susceptible to small near surface metal as its receivers are physically closer to the surface. However, as shown in Figure 5 the MetalMapper's late time measurements attenuate the responses of small scrap, while responses from larger, slow-decaying targets remain detectable. The late time MetalMapper detection data is therefore ideally suited to the primary objective of detecting 155 mm projectiles. Figure 6 shows polarizabilities extracted from four likely TOI targets identified in the late-time detection data. All of these items are a good match to large targets of interest in the ordnance library.

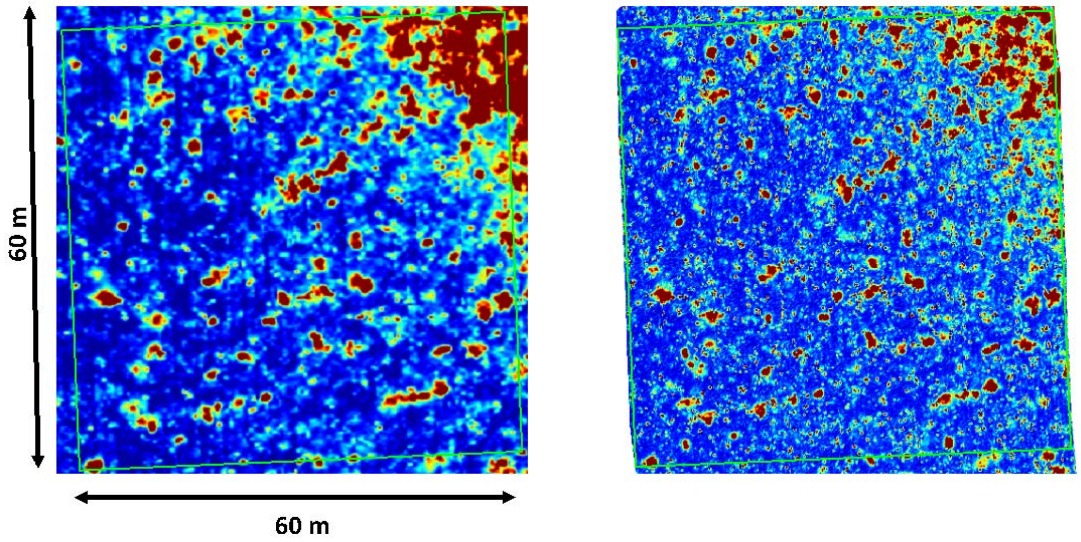

Figure 4. Left: EM61 Detection Data in Ft. Ord grid 11-B at 1.26 ms. Right: Dynamic MetalMapper Data at 1.24 ms, Collected Over the Same Area.

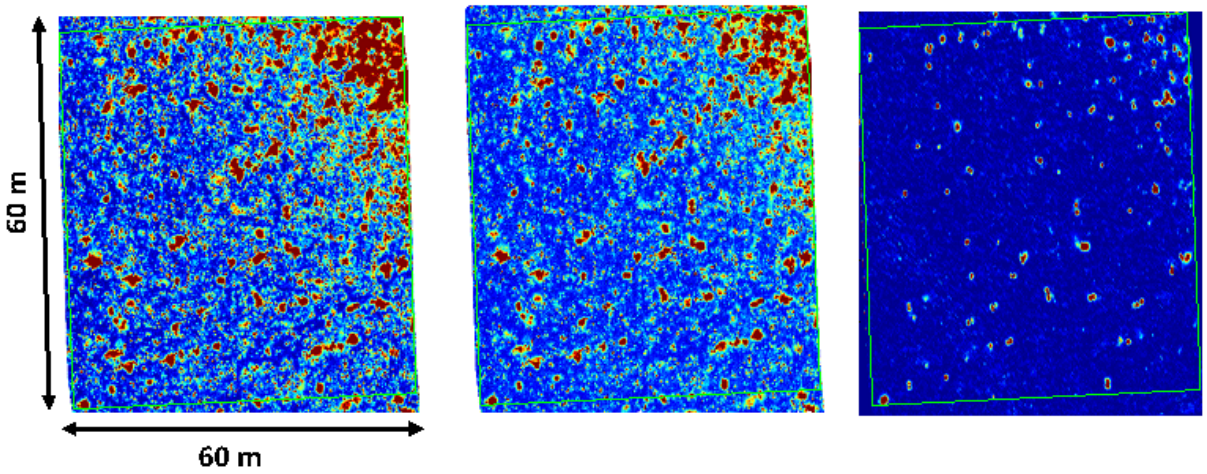

Figure 5. MetalMapper Detection Data in Grid 11-B at 0.63 ms (left), 1.23 ms (middle), 9.2 ms (right).

The northeast corner appears highly cluttered at early times but reveals distinct individual targets at later times.

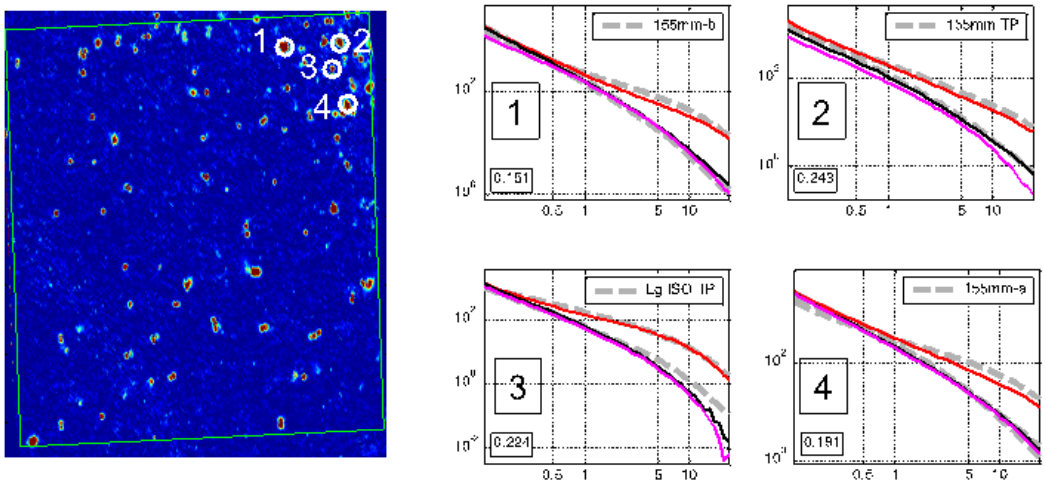

Figure 6. Left: MetalMapper Detection Data in Grid 11-B at 9.2 ms. White Circles and Numbers Indicate the Target Picks shown on right. Right: Estimated Polarizabilities (solid lines) Recovered from Cued Inversions for the Indicated Targets. Dashed Lines are the Best Matching Library Polarizabilities.

We picked targets in the MetalMapper dynamic data using vertical component profiles in all seven receivers. A separate worst-case detection threshold was calculated for each receiver, and initial picks from individual profiles were subsequently merged using a minimum anomaly footprint determined using the UXOLab detection modeler. Table 1 summarizes the total number of picks in each of the four MetalMapper grids.

Table 1. Summary of Target Picks in MetalMapper Grids.

Area	Density of metallic debris	Target picks	Average target picks per 100 ft subgrid
12A	Low	1698	283
12B	Medium	1878	470
11A	High	3646	608
11-B	High	3173	793

Page Intentionally Left Blank

4.0 CUED METALMAPPER PROCESSING

4.1 FEATURE EXTRACTION

Cued data were acquired in four different grids (Table 2 and Figure 7) at anomalies picked from dynamic MetalMapper data. In addition, cued data were acquired at anomalies picked from EM61 data in the vicinity of grids 11-A and 11-B. The total number of targets for the entire dataset is 2803.

Table 2. Summary of Targets in Each Grid.

Grid 11-EM61 refers to data acquired at anomalies in the vicinity of grids 11-A and 11-B picked from EM61 data. Target densities are based on number of targets in the full coverage sub-grids, where all targets were cued. "Targets other" refers to potential TOI targets that were cued in all other sub-grids.

Grid	Density	Total targets	Targets full coverage	Targets other	Target density (per acre)
12-A	Low	403	272	131	1186
12-B	Medium	494	417	77	1813
11-A	High	823	653	170	2831
11-B	Highest	934	790	144	3428
11-EM61	High	150	NA	150	NA

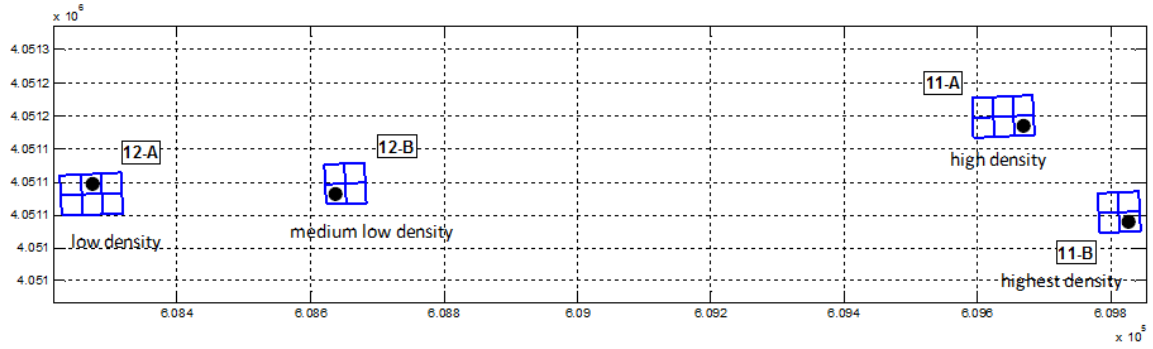

Figure 7. Relative Location of the Four Grids in which MetalMapper Data Were Acquired at Fort Ord.

Blue lines are outlines dividing each grid into either four or six 100×100 foot sub-grids. Black dots indicate sub-grids in which all anomalies were cued. Within the other sixteen sub-grids only anomalies previously identified from inversion of dynamic MetalMapper data as potential TOI were cued.

MetalMapper cued data for all anomalies were received as a set of TEM files for the cued anomaly data, background measurements and IVS and test pit measurements. TEM files were converted to CSV using TEMPlot (EM3DPlot). CSV files were imported into *UXOLab*.

On import *UXOLab* automatically performs background corrections, using the background that was collected closest in time for each anomaly. The data were inverted in *UXOLab* using a sequential inversion approach to estimate target location, depth and primary polarizabilities. Instrument height above the ground was assumed to be 12 cm. Noise standard deviation estimates were based on more than 80 background measurements. Target location was constrained to lie between ±0.75 m in both X and Y directions relative to the acquisition location. Target depth was constrained to lie between –1.3 and 0 m. The initial optimization for target location identified up to eight starting models to input into the subsequent estimation of polarizabilities. We performed three inversions per anomaly, solving for (1) a single object (single object inversion: SOI); (2) two objects (2OI); and (3) three objects (3OI).

Analysis of the data, including visual QC of data and model parameters, selection of training data, and dig list creation, was performed using the *UXOLab* software suite. Visual QC of the data was performed using the *UXOLab* module *QCZilla*, which provides a thorough overview of the observed and predicted data, predicted model parameters, and measures of data/model quality. Predicted polarizabilities were compared to reference polarizabilities for various ordnance items initially derived from IVS and test pit measurements. The Fort Ord IVS comprised only three items: small, medium and large ISOs. Test pit measurements were made over several items, including 40mm, 57mm, 60mm, 75mm, 81mm, several variants of 155mm, 2.36" rocket, Stokes mortar, and ISOs. As the analysis proceeded, the library of reference items was augmented with additional items based on a comparison with TOI from previous live sites, and from ground truth obtained through training data requests and partial ground truth. Each item in the ordnance reference library was assigned a size (diameter) in mm. Each item with a dig decision of "dig" in the submitted dig list was assigned a size category (1 for diameter <50mm; 2 for 50<diameter<=100mm; and 3 for diameter>100mm) based on the ordnance item in the reference library with the best matching primary polarizability (L1).

During data/model QC the primary objectives were to (1) flag high-likelihood TOI anomalies; (2) flag anomalies to be requested as training data; and (3) fail bad models and inversions. Anomalies flagged as high-likelihood TOI were monitored during the dig list creation phase to ensure they were being dug, ideally early in the dig list. Models and inversions were considered to be bad when the inversion failed (i.e., the data misfits are large), or when the recovered model location(s) were on, or near, an inversion boundary (i.e., significantly outside the footprint of the sensor). Bad models and inversions were identified in a semi-automated manner. E.g., models would be sorted by different measures of polarizability/data quality and the visual QC process would focus on the models with the poorest quality.

With multi-object inversions it is not uncommon that one of the models is unrealistic (e.g., deep, large in magnitude, sometimes located on or near a horizontal inversion boundary) yet provides the best fit to the reference polarizabilities (e.g., Figure 8). In such cases the model was flagged as failed. Models flagged as failed were not used in the classification process. Anomalies with all models from all inversions failed were classified as "cannot extract reliable parameters"; these anomalies were dug. For the Fort Ord dataset, ten anomalies (FO-10493, 25094, 25577, 35250, 35296, 36056, 40023, 40040, 40225 and 40263) were classified as "cannot extract reliable parameters". An example is shown in Figure 9. For a given anomaly, if more than one model was passed the classification procedure will consider all passed models and effectively use the one that is "best" based on the classification metric.

For anomalies with recollects, the classification procedure will consider all passed models from all versions of the anomaly and use the one that is “best” based on the classification metric.

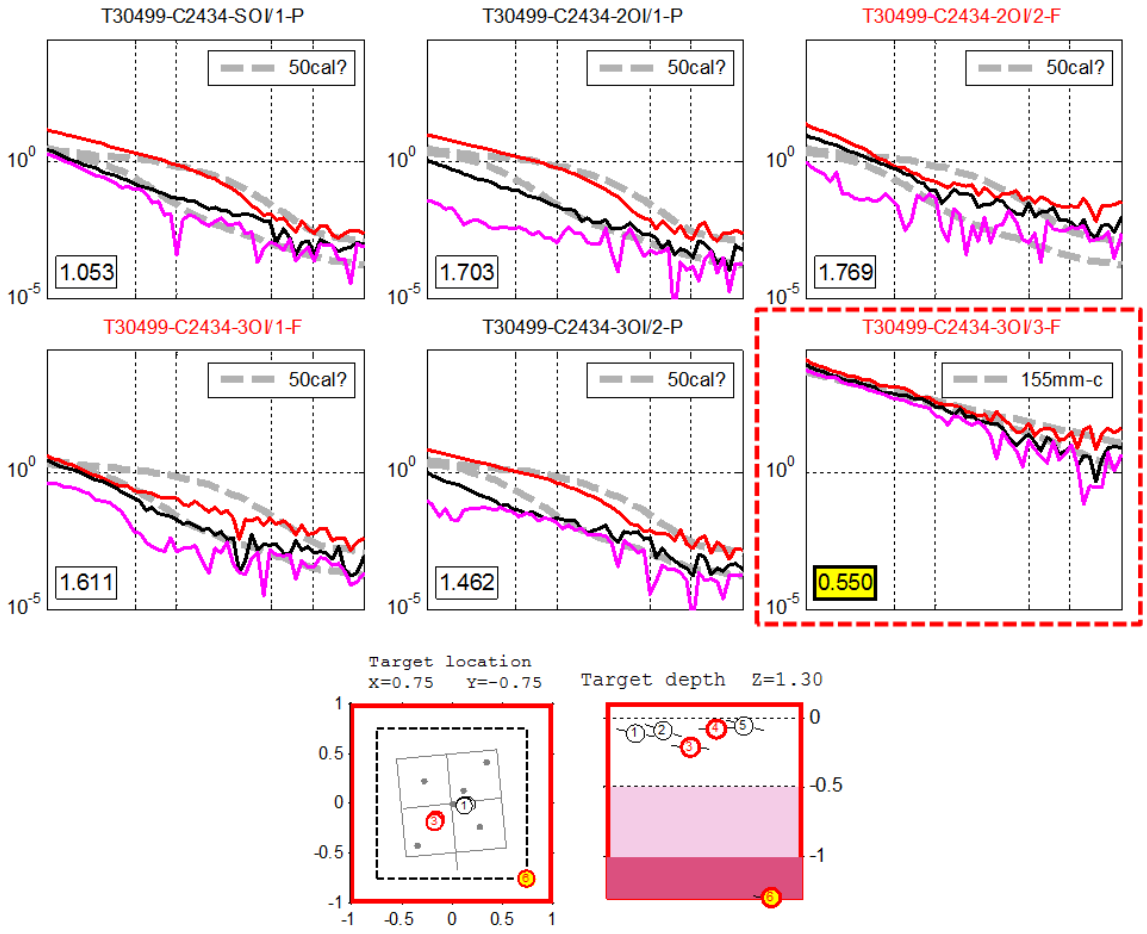

Figure 8. Example of an Unrealistic Model (FO-30499; frag).

Top row shows models from SOI and 2OI; middle row shows models from 3OI. For models 6 (box with broken red lines) the predicted depth is 1.3m and the predicted horizontal location is at a corner of the inversion boundaries. The polarizabilities for these models are high in amplitude and have a jittery appearance; classic signs that the model is an artifact of the multi-object inversion process. Accordingly, this model was failed during QC. Lower left plot shows predicted model locations (number circles) relative to the instrument receivers (grey lines) and transmitters (grey dots). Broken black line denotes the horizontal inversion bounds. Plot at lower right shows predicted model depths (numbered circles). The yellow highlighted circle in both plots at the bottom is model 6.

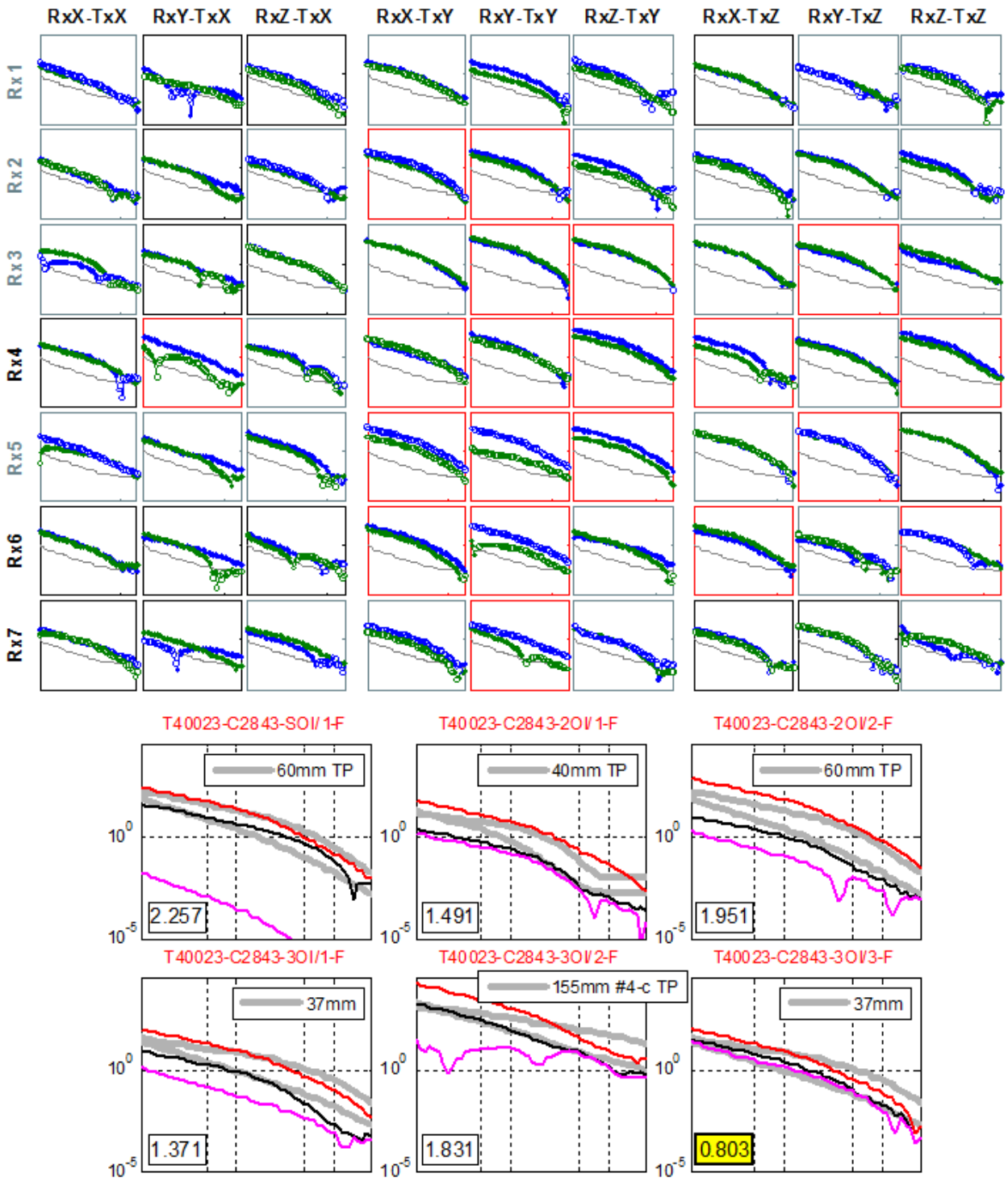

Figure 9. Example of an Anomaly with No Passed Models ("cannot extract reliable parameters"): FO-40023; large frag).

Top: data fits (blue = observed; green=predicted). Bottom: polarizabilities. The data fits for all inversions were very poor.

The Fort Ord MetalMapper Cued dataset comprised 2803 unique anomalies. Of the 21696 total models (including models from recollects), 13107 were passed and used in the classification process; 8589 were failed. Initially, 446 anomalies were classified as "high likelihood UXO" during QC, though some of these correspond to shared anomalies. Of the 446, about 375 correspond to unique locations. 370 of these (83%) correspond to TOI, though several of these are shared targets. The total number of unique TOI in the MetalMapper Cued dataset, excluding shared targets, is 356.

4.2 CLASSIFICATION

4.2.1 Training data selection

Figure 10 shows the distribution of models in decay versus size feature space. The overlap between the majority of features and reference items suggests that this may be a challenging site for classification because a relatively large proportion of the non-TOI will have size/decay characteristics similar to the TOI. Our *ad hoc* dataset degree of difficulty measure, which is based on various polarizability and dataset metrics, for this site suggests it will be significantly more difficult than previous ESTCP demonstrations at MMR and Beale, but easier than Rucker and New Boston.

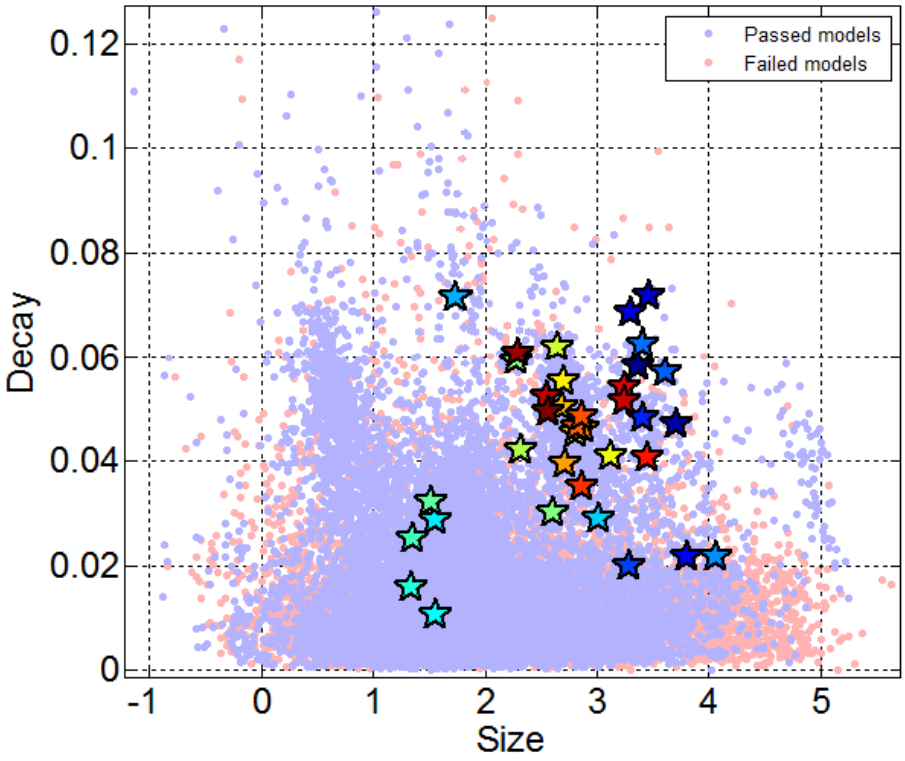

Figure 10. Distribution of Models in Decay(t75,t1) versus Size(t1) Feature Space¶where size(t1) is the total polarizability measured at the first time channel (t1=0.117 ms), and decay(t75,t1) is size(t75)/size(t1) where t75=5.232 ms. Some outliers are not shown. Stars represent selected ordnance library reference items ranging in size from 37mm to 155mm.

Our classification method is based on polarizability matching with respect to ordnance items in a reference library. For this approach to be successful it is important to determine the types of ordnance present at the site. During visual QC the analyst keeps track of suspicious, UXO-like items (i.e., items with modeled polarizabilities possessing UXO-like properties). Training data for some of these, particularly those with polarizabilities that are somewhat different from the items in the reference library, would be requested. In addition, we used our custom training data selection tool, *TrainZilla*, to explore feature space and automatically search for clusters of items with self-similar polarizabilities. In *TrainZilla*, the user selects a region in feature space by drawing a polygon, and the program automatically identify clusters of self-similar feature vectors by computing a misfit matrix **M** with elements

$$M_{jk} = \sum_{i=1}^{N} (L^{j}{}_{total}(t_i) - L^{k}{}_{total}(t_i))^2$$

where L^{j}_{total} is the log-transformed total polarizability for the j^{th} feature vector. Feature vectors with mutual misfit less than a user-specified threshold define a cluster in polarizability space. This analysis is helpful for identifying clusters that may not be readily evident in decay-size feature space: e.g., targets with consistent polarizabilities that may be hidden in the "cloud" of non-TOI features. A basic example of the use of *TrainZilla* is shown in Figure 11 and Figure 12.

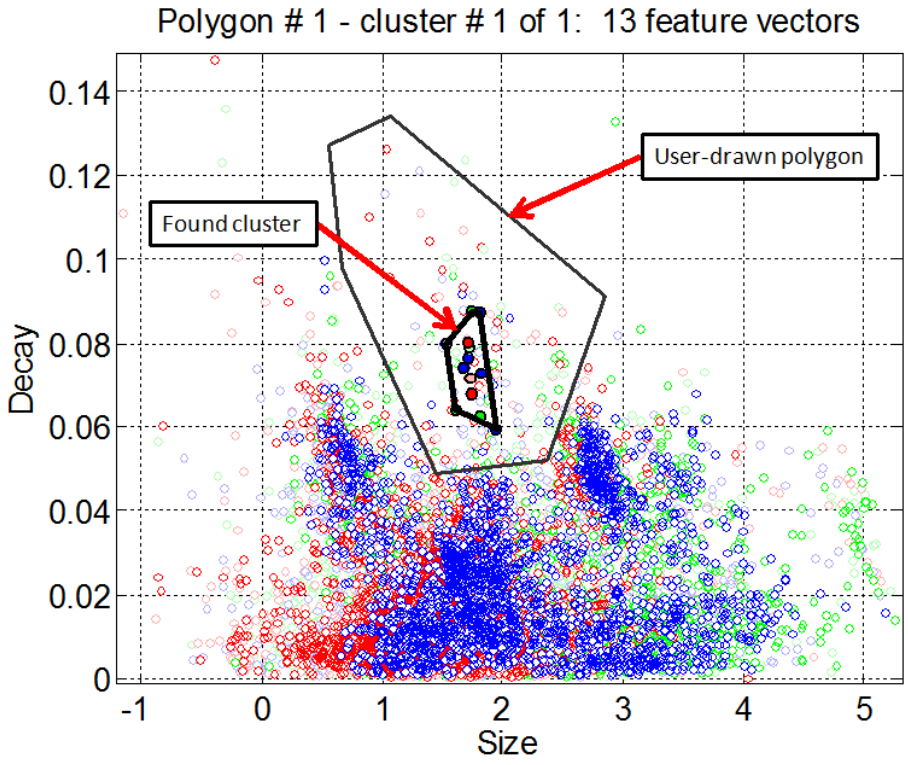

Figure 11. Example of Use of the Training Data Selection Tool (*TrainZilla*).

A polygon (solid black line) is drawn in feature space. Clusters of items with self-similar polarizabilities are automatically found based on the specified cluster search parameters. In this case a cluster comprising 13 features is visible (solid feature symbols encompassed by broken line). Polarizabilities for the models in this cluster are shown in Figure 12.

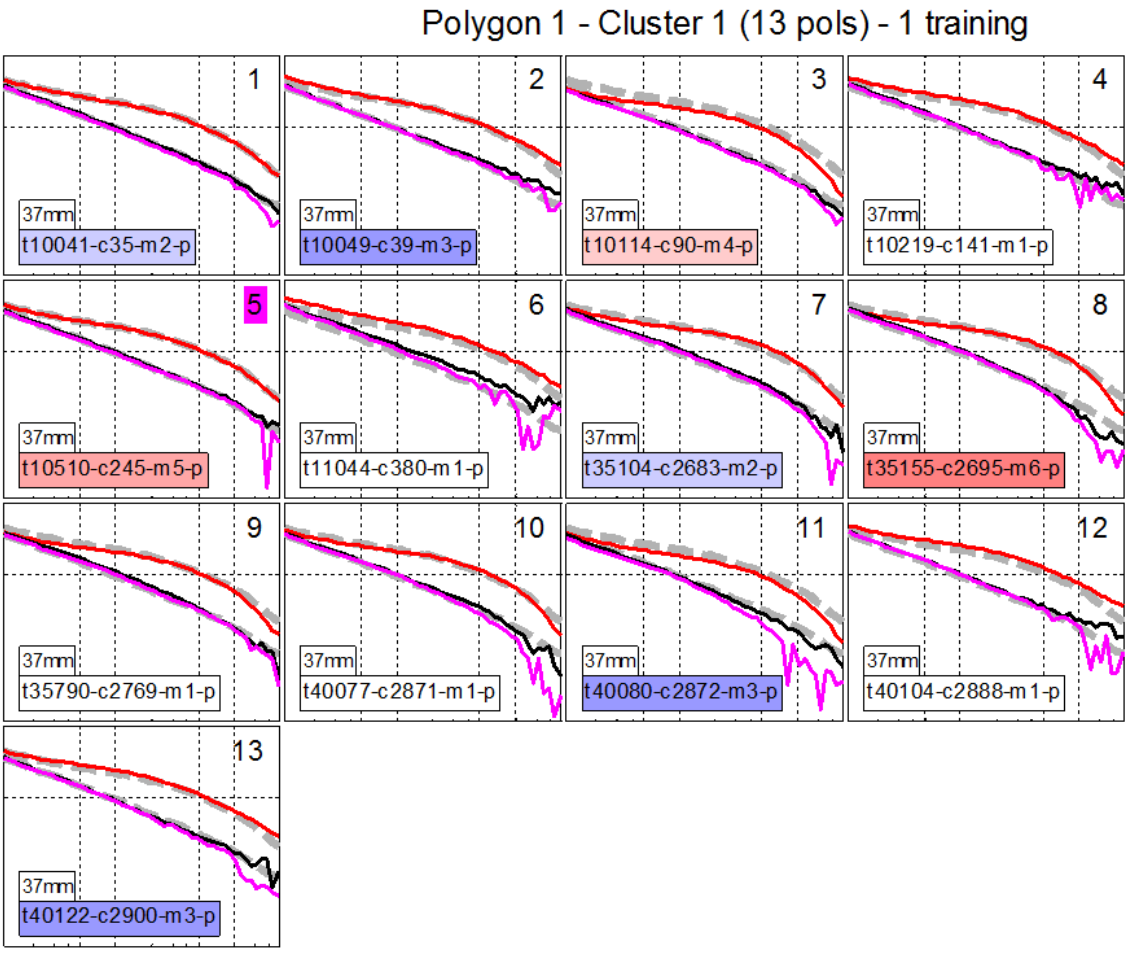

Figure 12. Polarizabilities for the Models in the Cluster Shown in Figure 11.

Red, black and magenta lines are predicted polarizabilities. Broken grey lines are best fitting reference polarizabilities. Target labels are number following "t" in the bottom label of each plot. Training data were requested for the 5th item (magenta-highlighted index number). This was confirmed to be a 37mm projectile (armor piercing tracer, M74). Subsequent ground truth information showed that all of these items are 37mm projectiles.

Our training data requests typically focus on: (1) items whose polarizabilities exhibit UXO-like properties distinct from those of items in our reference library; (2) items with polarizabilities similar to items in our reference library, but with degraded quality; (3) items from a cluster that do not necessarily have UXO-like properties but are from an unknown source; and (4) one-off items.

An alternative approach to selecting training data, and more one suited to finding potential one-off items, is to look for items with polarizabilities that closely match items in a large ordnance library. We do this with the UXOLab module called the Ordnance Museum (Figure 13), which, for MetalMapper cued data, comprises polarizabilities for approximately 470 items (ranging in size from 20mm to 155mm) from past ESTCP live site demonstrations. Approximately 240 of these items were derived from the UX-Analyze polarizability library. With the Ordnance Museum we can easily search for models in our dataset with polarizabilities similar to any of the museum items.

For Fort Ord we found several items with close matches (polarizability misfit < 0.3 calculated using all three polarizabilities) to Ordnance Museum items. Four representative items are shown in Figure 14. We requested training data for all of these items; one of these was a TOI.

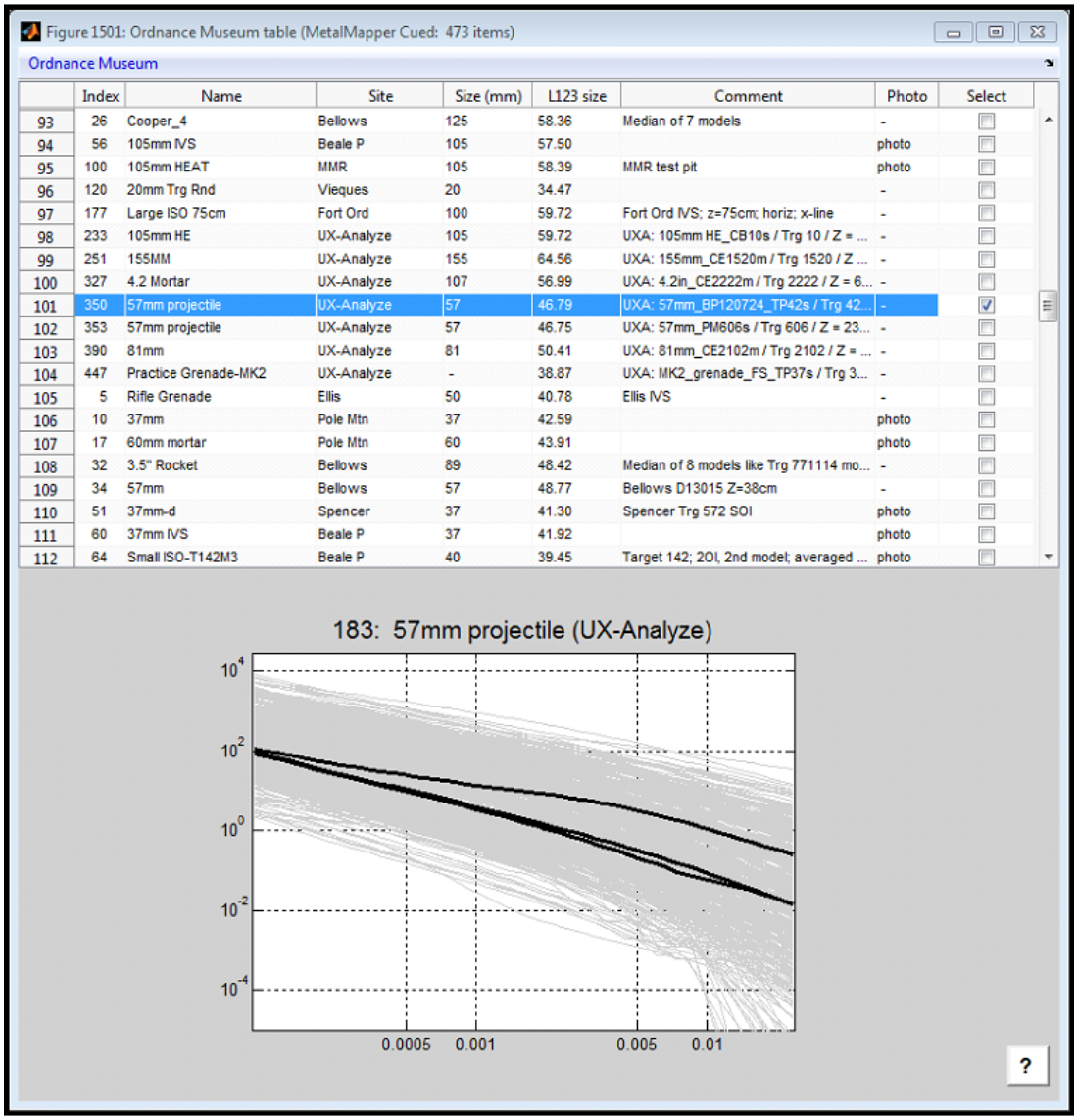

	Index	Name	Site	Size (mm)	L123 size	Comment	Photo	Select
93	26	Cooper_4	Bellows	125	58.36	Median of 7 models	-	
94	56	105mm IVS	Beale P	105	57.50		photo	
95	100	105mm HEAT	MMR	105	58.39	MMR test pit	photo	
96	120	20mm Trg Rnd	Vieques	20	34.47		-	
97	177	Large ISO 75cm	Fort Ord	100	59.72	Fort Ord IVS; z=75cm; horiz; x-line	-	
98	233	105mm HE	UX-Analyze	105	59.72	UXA: 105mm HE_CB10s / Trg 10 / Z = ...	-	
99	251	155MM	UX-Analyze	155	64.56	UXA: 155mm_CE1520m / Trg 1520 / Z ...	-	
100	327	4.2 Mortar	UX-Analyze	107	56.99	UXA: 4.2in_CE2222m / Trg 2222 / Z = 6...	-	
101	350	57mm projectile	UX-Analyze	57	46.79	UXA: 57mm_BP120724_TP42s / Trg 42...	-	☑
102	353	57mm projectile	UX-Analyze	57	46.75	UXA: 57mm_PM606s / Trg 606 / Z = 23...	-	
103	390	81mm	UX-Analyze	81	50.41	UXA: 81mm_CE2102m / Trg 2102 / Z = ...	-	
104	447	Practice Grenade-MK2	UX-Analyze	-	38.87	UXA: MK2_grenade_FS_TP37s / Trg 3...	-	
105	5	Rifle Grenade	Ellis	50	40.78	Ellis IVS	-	
106	10	37mm	Pole Mtn	37	42.59		photo	
107	17	60mm mortar	Pole Mtn	60	43.91		photo	
108	32	3.5" Rocket	Bellows	89	48.42	Median of 8 models like Trg 771114 mo...	-	
109	34	57mm	Bellows	57	48.77	Bellows D13015 Z=38cm	-	
110	51	37mm-d	Spencer	37	41.30	Spencer Trg 572 SOI	photo	
111	60	37mm IVS	Beale P	37	41.92		photo	
112	64	Small ISO-T142M3	Beale P	40	39.45	Target 142; 2OI, 2nd model; averaged ...	photo	

Figure 13. *UXOLab Ordnance Museum* Interface.

This is a library of reference polarizabilities compiled from several ESTCP live site demonstrations, and other projects. The ordnance museum for MetalMapper Cued data currently comprises approximately 470 items ranging in size from 20mm to 155mm projectiles.

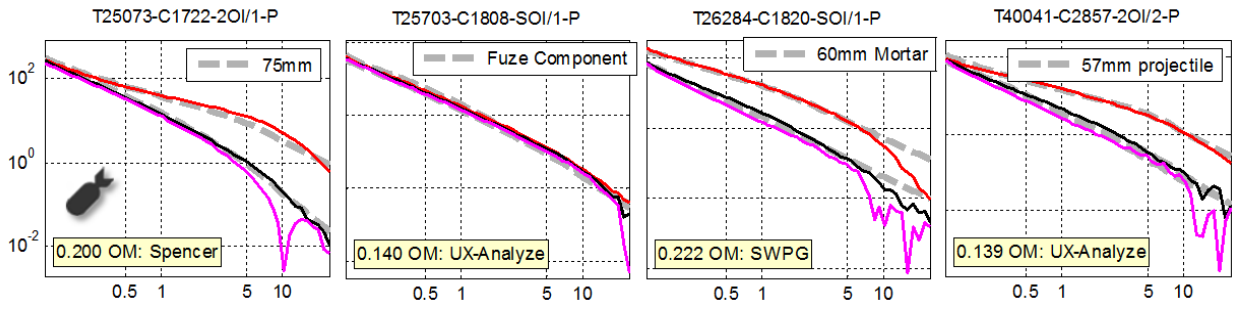

Figure 14. Polarizabilities of Four Models with Close Matches to Items in the *Ordnance Museum*.

Anomaly labels are the number following the "T" in each plot title. Label at top right of each plot is best fitting ordnance museum item name. Label at bottom left in each plot shows the polarizability misfit and source of the model. We requested training data for all of these items. The first was a TOI (75mm); the rest were non-TOI. The second item (FO-25703) was an M48 series fuze (non-TOI).

We submitted three training requests prior to submitting our first dig list for a total of 62 training items. Twenty-eight of these were TOI (37mm, 40mm, 57mm, 75mm, 81mm and 155mm). Based on our training data we removed a number of items from our working reference library, e.g., small ISO, Stokes Mortar, rockets (2.36" and 3.5") and fuzes.

4.2.2 Classification method

Dig lists were developed using our visual classification software *DigZilla* (Figure 22, which is fully integrated with other elements of the *UXOLab* software suite. *DigZilla* allows for the creation of multi-stage dig lists with minimal effort, and supports a number of classifiers.

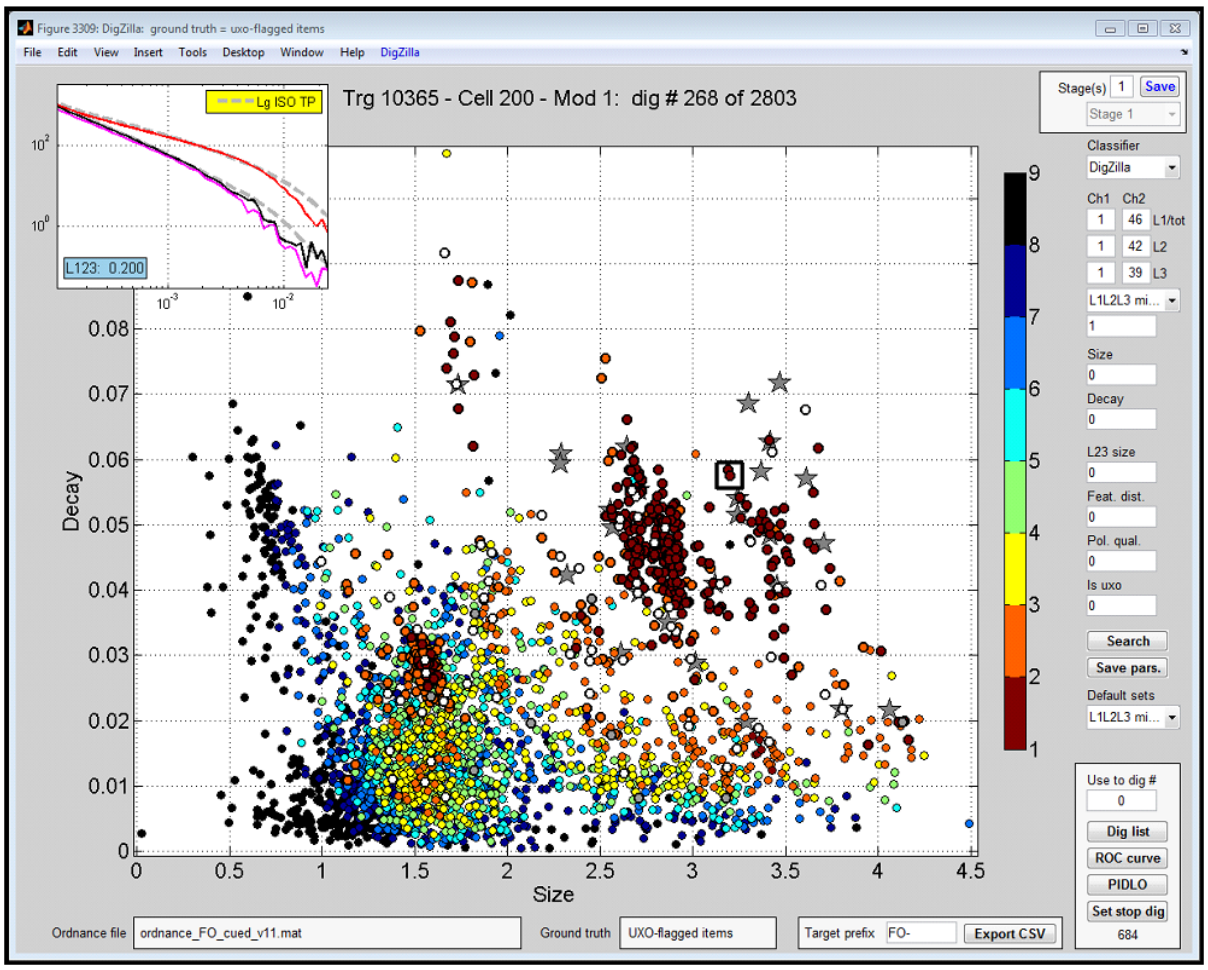

Figure 15. Screen Shot of the *UXOLab DigZilla* Graphical User Interface.

Features in the decay versus size feature plot are color coded according to dig list order (red earliest, black latest). White dots are training items. Stars are reference items. Inset polarizabilities at top left are for the currently selected item (black square).

We were informed by the ESTCP Program Office that the Fort Ord classification results would be scored twice: (1) for the primary objective of finding all large TOI (155mm projectiles and large ISOs) to a depth of 60 cm; and (2) detection of all munitions. Submission of two separate dig lists was permitted but not required. We chose to submit a single two-phase dig list. For the first phase we use a polarizability library comprising only large items (155mm and large ISO). For the second phase we use our full polarizability library (including the large items). For both phases, the classification approach was identical, based on polarizability misfit (to the best fitting library reference item for each model) using all three polarizabilities. Misfits were calculated between the first time channel (0.12 ms) and channels 46 (12.624 ms), 42 (8.284 ms) and 39 (6.038 ms), respectively for L1, L2 and L3. The end time channels for the misfits were determined automatically based on a measure of polarizability reliability. The ordnance library used for the first phase of the dig list (up to dig number 203) comprised 12 items; the full library used for the second phase comprised 35 items (Figure 16). The stop dig point for this list was dig number 667.

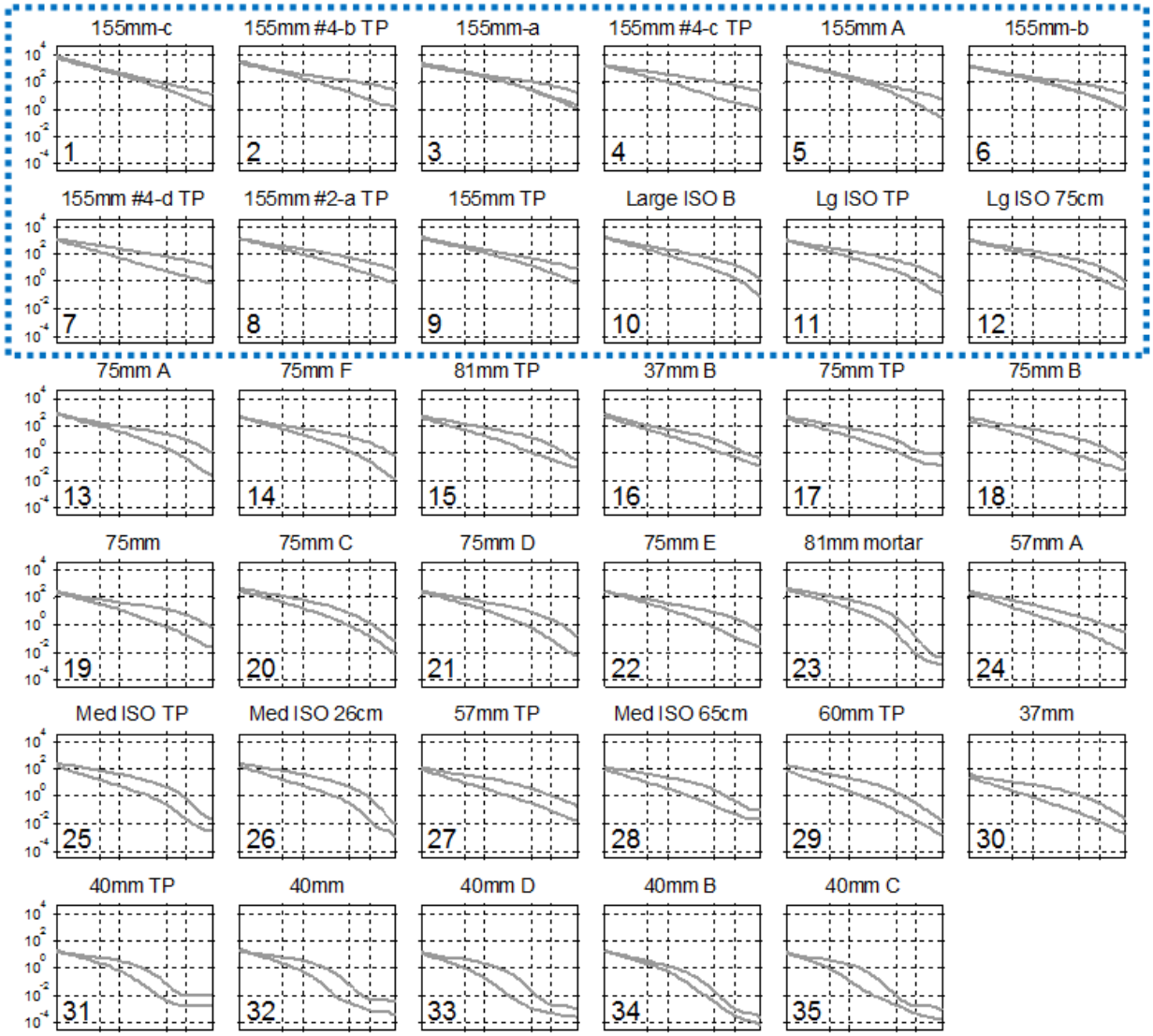

Figure 16. Items in the Ordnance Reference Library Used for the Stage 1 Dig List.

The first 12 items were used in the first phase of the dig list (up to dig number 203) for finding large TOI. The full library was used for subsequent digs.

The stage 1 dig list missed two QC seeds. The partial ROC curve is shown in Figure 17.

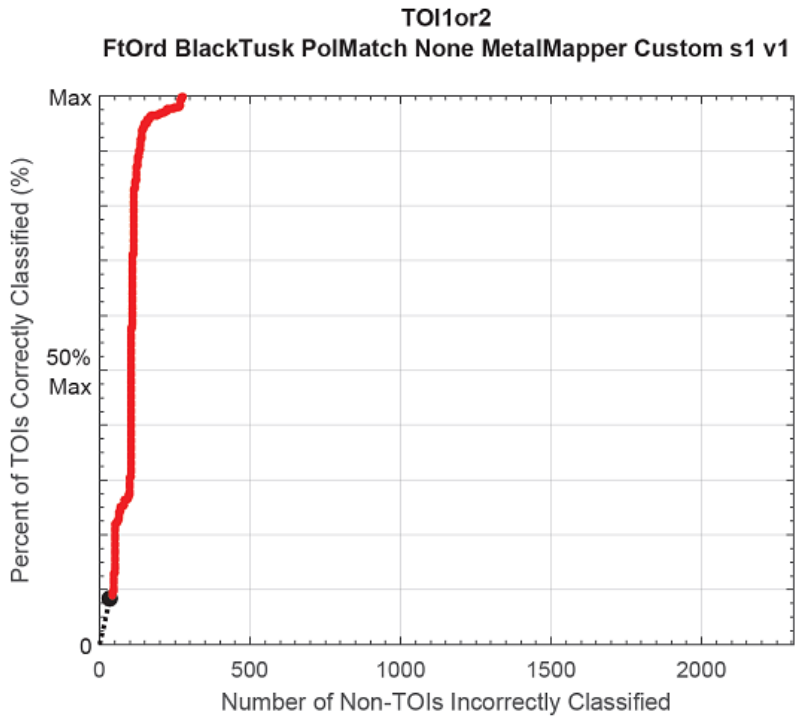

Figure 17. Partial ROC Curve for the Stage 1 Dig List.

Because two QC seeds were missed, we were required to submit a Failure Analysis Memo, which is presented below in its entirety. The memo describes actions taken to mitigate against missing TOI in the stage 2 dig list.

Failure Analysis Memo

Site: Fort Ord
Analyst: Black Tusk Geophysics
Data: MM Cued
Date: June 29, 2015

Our stage 1 dig list missed two QC seeds (Table 3).

Table 3. List of Missed QC Seeds.

Anomaly	Depth (cm)	Identification	Dig Number
FO-40248	26	Small ISO	726
FO-25074	30	Unidentified large TOI (75mm?)	2171

a. Analysis of the factors that resulted in the misclassification of each missed seed

FO-40248 (small ISO at 26 cm depth)
During the training portion of the data analysis, we specifically requested ground truth for several anomalies with excellent matches to the IVS and test pit small ISO polarizabilities (Figure 18). All of these were identified as non-TOI (frag). On this basis we removed the small ISO reference polarizabilities from our reference library and hence missed the QC seed.

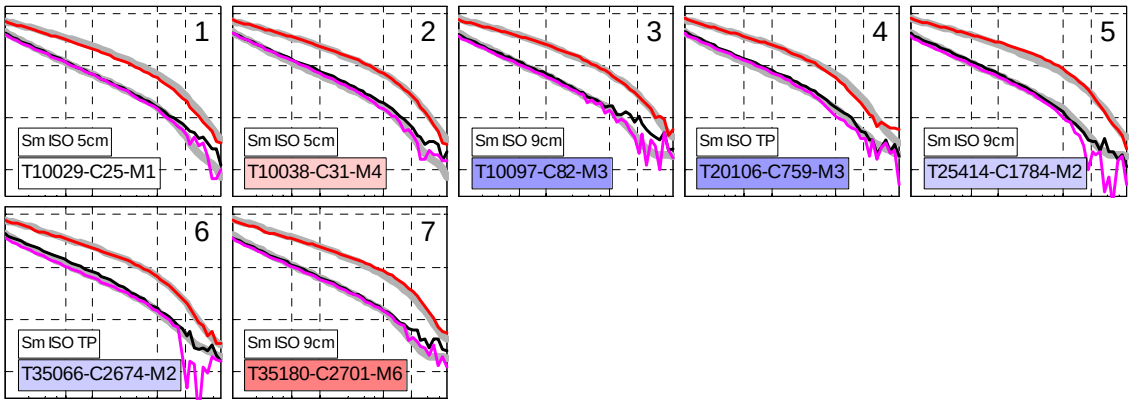

Figure 18. Polarizabilities for Seven Anomalies with Excellent Matches to Our Small ISO Reference Items (which were based on local IVS and test pit measurements).

We requested training data for all of these; all were identified as frag.

FO-25074 (75mm? at 30 cm depth)
This seed item was not identified in the ground truth file, but it appears to be a 75mm projectile. A re-inspection of the data for this anomaly (Figure 19) shows that several of the components have relatively large misfits. Ideally, this anomaly should have been classified as "cannot analyze". Its misfit metric was, however not quite large enough for this anomaly to be flagged for visual inspection for a decision to be made by the analyst. Thus, essentially this TOI was missed because the metric used for flagging poor data fits was not low enough, i.e., analyst error.

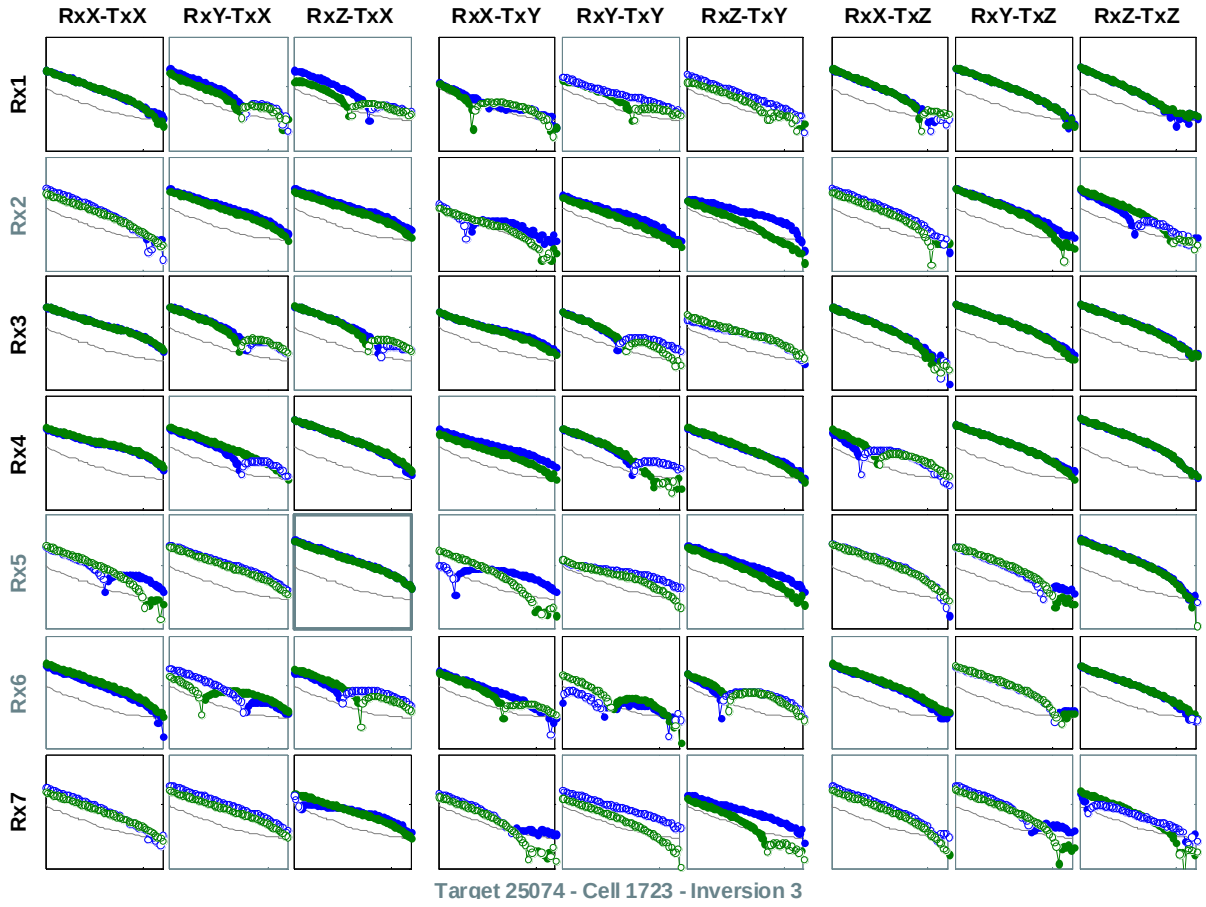

Figure 19. Data for Missed Seed FO-25074 (75mm).

Several components have large misfits and thus this anomaly should have been classified as "cannot analyze". Blue = observed data; green = predicted data.

b. Description of how the analysis procedures have been modified based on the additional information provided

We have re-inserted the small ISO reference polarizabilities into our reference library to ensure that all small ISOs with a good match to these items will be dug. We have also re-examined anomalies with large data misfits to looks for other cases of anomalies that should be classified as "cannot analyze". An additional 19 items were classified as "cannot analyze".

c. Evidence that the modified analysis scheme correctly classifies the missed seeds and can reasonably be expected to correctly classify all remaining TOI.

With the addition of the small polarizabilities into our reference library, the missed seed FO-40248 would have been dug because its polarizability misfit is 0.493, whereas we were digging all items with misfits less than 0.6. Without the small ISO polarizabilities in the reference library, its misfit was 0.624 (with a best match against a 37mm item), and hence was not originally dug. Other items with good matches to our small ISO reference items will now be dug.

We have also re-inspected items with poor misfits to ensure that anomalies with poor data fits from all inversions are classified as "cannot analyze".

In addition to the steps described in the above failure memo, we augmented our ordnance reference library with five new items based on the TOI found in the stage 1 dig list. For the stage 2 dig list we dug an additional 245 items. The stage 2 partial ROC curve is shown in Figure 20. Five more TOI were found. Three of these (FO-25021, 25129 and 50048) were anomalies which, after re-QC, were classified as cannot analyze. Of the remaining two, one (FO-40258) was a small ISO. The other (FO-25105) was a 75mm projectile.

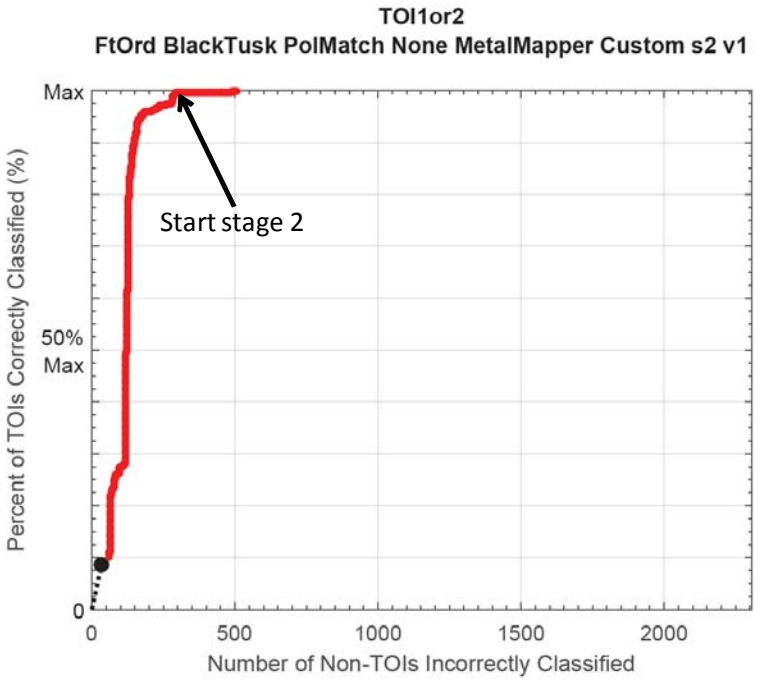

Figure 20. Partial ROC Curve for the Stage 2 Dig List.

After additional QC, one more anomaly was classified as cannot analyze. Inspection of the polarizabilities for the anomalies after the stop dig point of the stage 2 dig list revealed no remaining high-likelihood TOI. As a simulated quality assurance (QA) measure, we decided to select an additional 25 of the most likely anomalies (visually, based on polarizability shape and size) for digging in stage 3. Several of these looked like potential 40mm projectiles, but had polarizability misfits with respect to the 40mm reference items that were too large to result in them being placed on the dig list. The partial ROC curve for stage 3 is shown in Figure 21. No additional TOI were found.

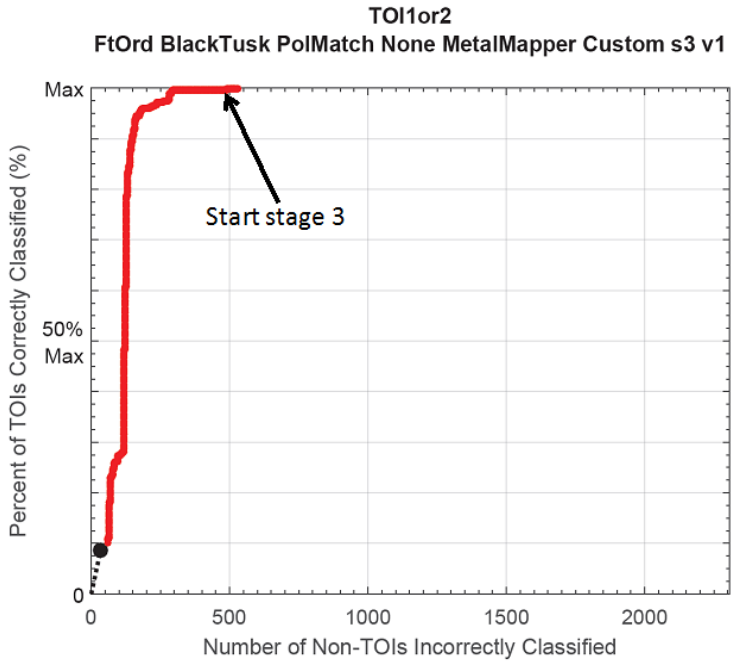

Figure 21. Partial ROC Curve for the Stage 3 Dig List.

With no additional TOI found in the stage 3 dig list, digging was terminated and the stage 3 list was declared to be the final dig list. Separate final scoring (Figure 22 and Figure 23) was received for the two objectives of this study (finding all large TOI to a depth of 60 cm, and detecting all munitions).

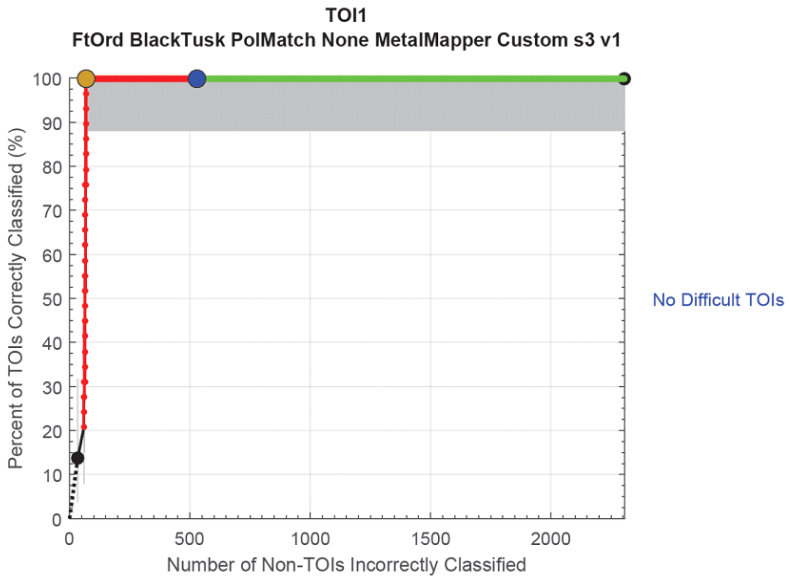

Figure 22. Final Scoring for Primary Objective (finding all large TOI to a depth of 60 cm).

Orange dot denotes location of last TOI. Blue dot is stop dig point.

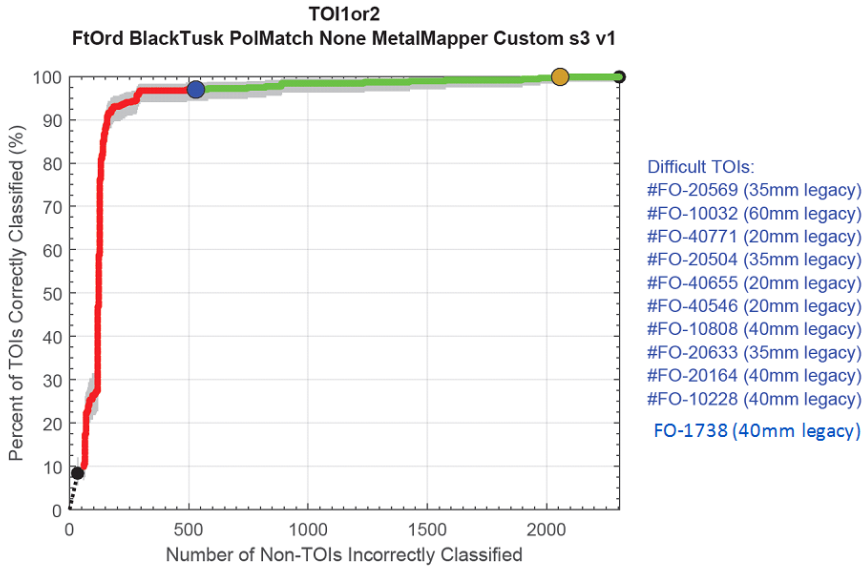

Figure 23. Final Scoring for Secondary Objective (detecting all TOI).

Eleven TOI occur after the stop dig point. Orange dot denotes location of last TOI. Blue dot is stop dig point.

The primary objective of finding all large TOI to a depth of 60 cm was easily achieved (Figure 22). Because we did not submit a dig list specifically tailored to finding only large TOI, the stop dig point on the final ROC curve in Figure 22 is the stop dig point that was used for finding all TOI. If the stop dig point were to be taken as the point in the first stage dig list where classification changed from specifically looking for large TOI only to looking for all TOI (dig #203), the stop dig point would occur 54 digs after the last TOI was found.

The secondary objective of finding all TOI was not achieved, with eleven TOI missed. Of the 356 unique TOI on site, we found 345 (96.9%) with 874 total digs of unique targets. Ignoring the eleven missed TOI, the false alarm rate was 1.53 non-TOI digs per TOI dig. Further analysis of the missed TOI is presented in the following retrospective analysis.

4.2.3 MetalMapper cued retrospective analysis

Our final dig list missed eleven TOI (Table 4): four 40mm projectiles, three 35mm subcaliber rockets, three 20mm projectiles, and one 60mm illumination round. We will look at each group of similar target types separately.

Table 4. List of Eleven Missed TOI Ordered by Dig Number.

All munitions except the 60mm illumination round are practice rounds.

Anomaly	Depth (cm)	Identification	Dig Number
FO-10738	19	40mm M918	989
FO-10228	2	40mm M918 (nose only)	1167
FO-20164	3	40mm M781 + frag	1251
FO-20633	10	35mm subcaliber rocket M73	1318
FO-10808	1	40mm M918 (nose only) + frag	1322
FO-40546	3	20mm M99	1688
FO-40655	6	20mm M99	1886
FO-20504	8	35mm subcaliber rocket M73	2045
FO-40771	12	20mm M99	2384
FO-10032	23	60mm illumination round M83	2459
FO-20569	12	35mm subcaliber rocket M73	2552

4.2.3.1 Missed TOI: 40mm (4: FO-10738, 10228, 20164 and 10808)

The four missed 40mm projectiles are shown in Figure 24.

Figure 24. Four Missed 40mm Projectiles.

Missed TOI FO-10738

As shown in Figure 25, the location of the excavated 40mm projectile is about 1.4 m east of the target pick and sensor location. In addition to the large offset, this item was located at a depth of 19 cm. Of the 89 40mm projectiles recovered during this project, this was the greatest depth found. Given the very large offset, relatively deep depth, and small size of the target, it is not surprising that this TOI was missed. Furthermore, as shown in Figure 25, our results suggest that, with very little doubt, a 50 caliber projectile is located at the target pick location of FO-10738, yet the ground truth information makes no mention of this. Our conclusion for this anomaly is that (a) the 40mm projectile should not be associated with this anomaly; and (b) the ground truth information is suspect because it did not report finding a 50 caliber projectile at the target pick location.

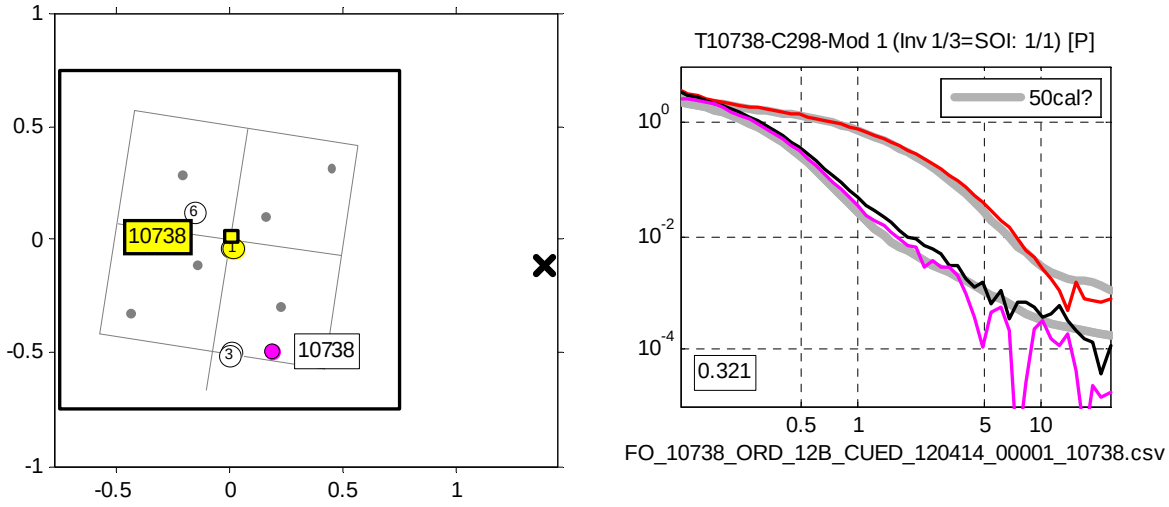

Figure 25. Left: Sensor and Ground Truth location for Missed TOI FO-10738 (40mm). Right: Polarizabilities for the Single Object Inversion Show that a 50 Caliber Projectile is Almost Certainly Located at the Target Pick Location (at a depth of ~3 cm), Yet the Ground Truth Information Has No Mention of This.

Left: Labeled yellow square is target pick location for FO-10738. Light grey lines and dots show location of MetalMapper transmitters and receivers (short grey line point south shows that front face of the sensor is facing south). Numbered white and yellow circles are predicted model locations from single and multi-object inversions. Broken black line shows extent of inversion bounds (predicted models are constrained to lie within these bounds). Labeled magenta dot is location of a recollect. Black x shows ground truth location of the 40mm projectile, which is approximately 1.4 m east of the target/sensor center.

Missed TOIs FO-10228 and 10808

Both of these are nose parts only of a 40mm projectile. We had encountered a 40mm nose part in our stage 1 dig list and the polarizabilities from this item (FO-10372) were added to our reference library. The polarizabilities for FO-10229 and 10808 (Figure 26) show a distinct resemblance to the 40mm nose reference polarizabilities, however, the misfit values (0.711 and 1.171, respectively) were larger than our stop dig threshold (0.6) and so these items appeared after the stop dig point. The 40mm nose part is the smallest item in our reference library, and in retrospect it is clear that there is significant variation in the polarizabilities for this item.

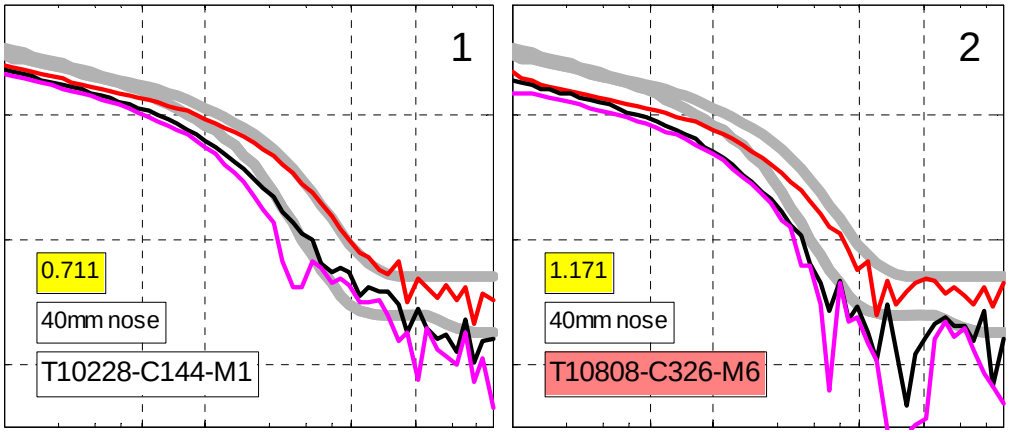

Figure 26. Polarizabilities for Missed 40mm Projectiles FO-10228 (left) and FL-10808 (right).

Both are nose parts only, and both show similarities with our 40mm nose reference polarizabilities (broken grey lines); however, the misfit values (yellow labels) were large enough that these items appeared after the stop dig point.

Missed TOI FO-20164

The 40mm projectile at anomaly FO-20164 can be considered a "one-off": it is an M781 type practice round, while all other 40mm projectiles classified as TOI for this study are M918 type. The 88 M918 TOI were all found in Grids 12A and 12B, while a total of 19 M781 types were found, all in grid 11-B; however only one of these (FO-20164) is classified as a TOI in the ground truth. In fact we did receive training data for an M781 type 40mm: FO-20446, however (a) it was classified as MD, and (b) its polarizabilities were distinctly different from those of FO-20164. The polarizabilities for FO-20446 are essentially identical to the 40mm nose polarizabilities from our reference library.

The M781 is smaller than the M918. We also note that the projectile was actually located about 1.3 m SW from the target pick for FO-20164. FO-20164 was acquired a total of 6 times. The sixth acquisition was only about 25 cm from the projectile, so that the projectile was well within the footprint of the sensor. The polarizabilities for FO-20164 (Figure 27) are distinct from all the 40mm polarizabilities in our reference library. This is a classic example demonstrating the difficulty in finding distinct, small one-off items.

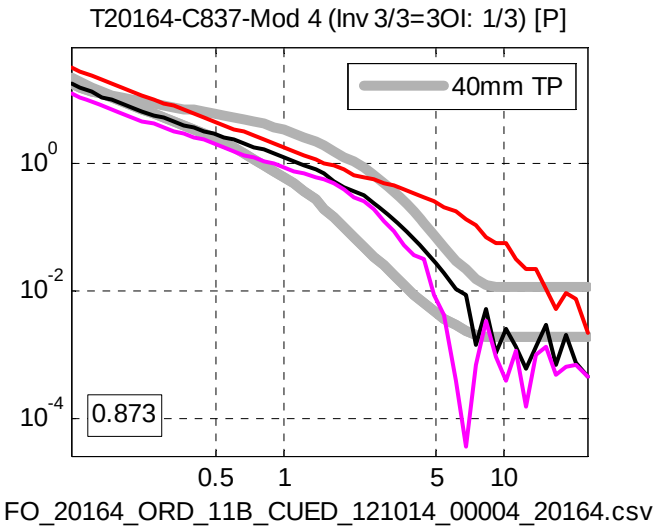

Figure 27. Polarizabilities for Missed 40mm Projectiles FO-20164.

Broken grey lines are for a reference 40mm measurement made at the test pit. This item is a one-off M781; all other 40mm TOI found during this study are the larger M918 type.

4.2.3.2 Missed TOI: 35mm subcaliber rockets (3: FO-20633, 20504 and 20569)

The three missed 35mm subcaliber rockets are shown in Figure 28. While these three items look identical, the recovered polarizabilities vary significantly, hence there was no chance of identifying these as belonging to a small cluster. For comparison purposes we will use the polarizabilities from FO-20504 as a reference for the 35mm rocket. The rocket at this anomaly is the most shallow of the three, and the only one where a piece of scrap was not found along with the TOI. But even for FO-20504, it is not clear which, if any of the models, are truly representative of the 35mm rocket. We use one of the models from the 2-object inversion for the following retrospective analysis.

Figure 28. Three Missed 35mm Subcaliber Rockets.

Missed TOI FO-20633

A large conical fuze, resembling an M54 fuze (for example found at Camp Beale), was found at this location in addition to the 35mm rocket. The fuze was found a more shallow depth (8 versus 10 cm) and is closer to the center of the sensor (3 versus 27 cm). Recovered polarizabilities for this anomaly (Figure 29) show that the reference item with the best fit is an M54 fuze. The predicted location and depth for these models are consistent with the fuze that was found. None of the other models resembles the 35mm reference polarizabilities taken from FO-20504. Note that the M54 reference item shown in Figure 29 was not used in the reference ordnance library used for classification because fuzes were not considered TOI.

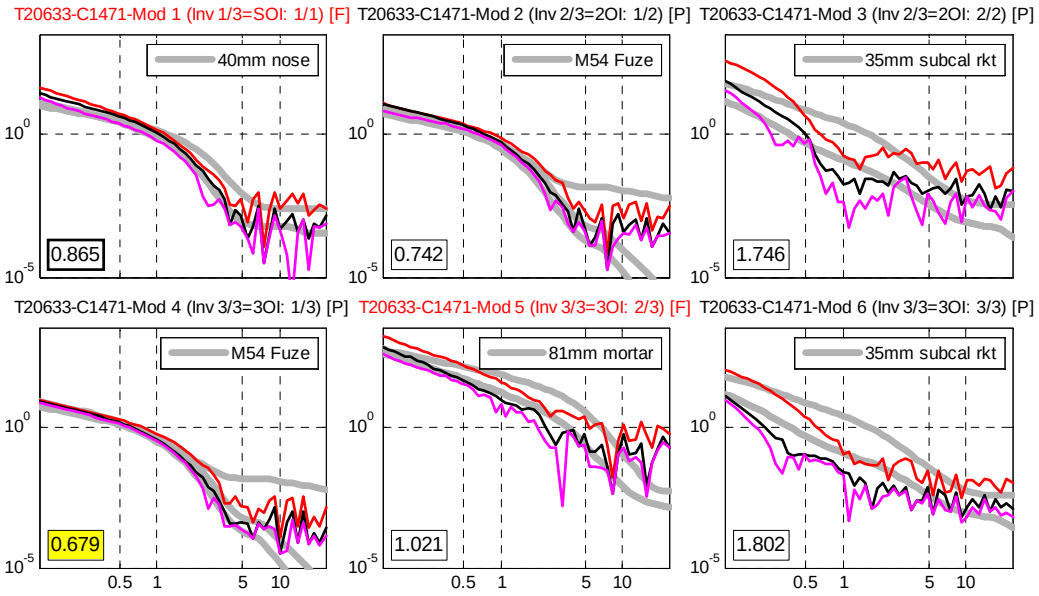

Figure 29. Polarizabilities for All Six Models of FO-20633 (missed 35mm subcaliber rocket) Along with the Best Fitting Polarizabilities from the Reference Library (broken grey lines).

Note that one of the models (lower left) is a close match to an M54 fuze. A fuze that looks like an M54 was also found at this anomaly location. None of the polarizabilities match those from FO-20504. Top row: models for 1- and 2-object inversions; bottom row: models for 3-object inversion. Numbers in lower left are misfit values between observed and reference polarizabilities (smaller number implies better fit).

Missed TOI FO-20504

Of the three missed 35mm rockets, this was the most shallow (8 cm), closest to the center of the sensor (3 cm offset), and the only one not accompanied by a piece of scrap. In theory this item should produce the most representative set of polarizabilities for the 35mm rocket, hence we are using one of the models from this anomaly as the de-facto reference for the 35mm rocket in this retrospective analysis. Typically when a model can be well constrained, the polarizabilities for the single object inversion, and the polarizabilities from one model each of the 2- and 3-object inversions should all look similar. In this case that is not true as can be judged by the large misfit values for all but the second model in Figure 30. The reference polarizabilities based on FO-20504 are actually fairly typical of small scrap, hence the difficulty in finding this TOI (e.g., Figure 31).

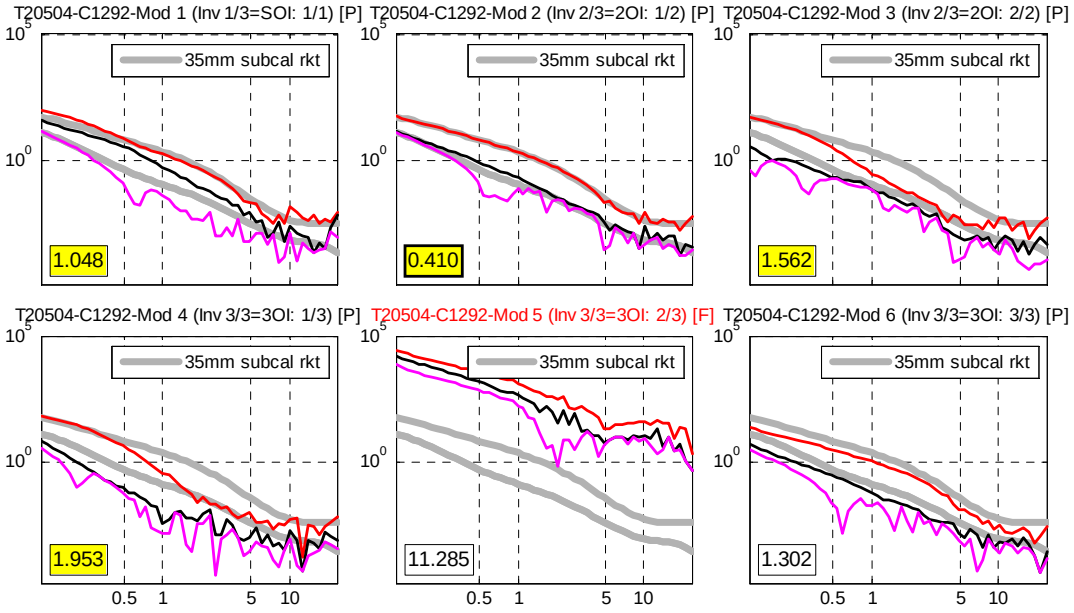

Figure 30. Polarizabilities for All Six Models of FO-20504 (missed 35mm subcaliber rocket).

The reference polarizabilities (broken grey lines) are based on the second model (top row, center). Note the inconsistency of the models. Top row: models for 1- and 2-object inversions; bottom row: models for 3-object inversion. Numbers in lower left are misfit values between observed and reference polarizabilities (smaller number implies better fit).

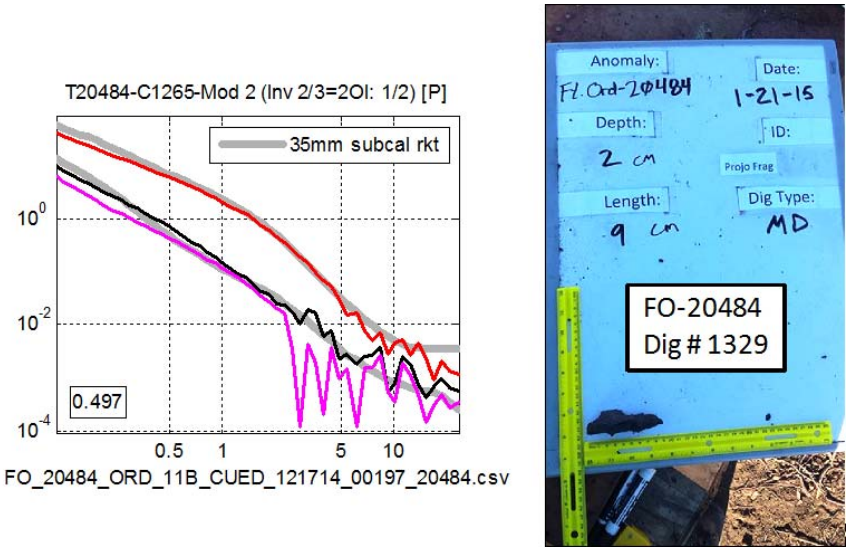

Figure 31. Polarizabilities for FO-20484 (small frag) Plotted Against the Polarizabilities for FO-20504 (missed 35mm rocket TOI; broken grey line).

This illustrates how the 35mm rocket is basically indistinguishable from small frag.

Missed TOI FO-20569

This 35mm rocket was challenging because it was located outside the footprint of the sensor (Figure 32), at an offset of 59 cm from the center of the sensor. It is the deepest of the three missed 35mm rockets and there is a small piece of frag closer to the center of the sensor (12 cm offset) at a depth of only 2 cm. One of the 3-object inversion models (model 6) is located near the position of the rocket, but the polarizabilities for this model (Figure 33) are very dissimilar to the reference polarizabilities based on FO-20504. None of the other models are a good match, either. It is most likely that models 2 and 5 represent the small frag. It seems that, because of its position, depth and relatively small size, the rocket is not resolved by the data.

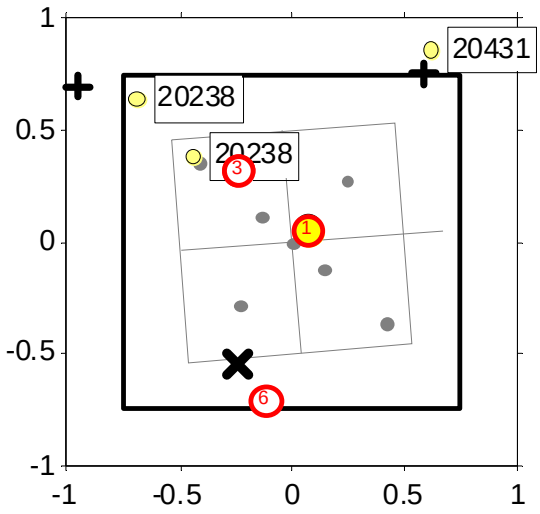

Figure 32. Ground Truth Location of the 35mm Rocket at FO-20569 ("X") versus Sensor Location (light grey lines and dots show MetalMapper transmitters and receivers).

Note that the rocket lies outside the footprint of the sensor (59 cm from center of sensor). Numbered circles are the predicted model locations for the three inversions. Model 6 (just below the X) is the model nearest to the rocket, but its polarizabilities are a very poor match to the reference polarizabilities for a 35mm rocket.

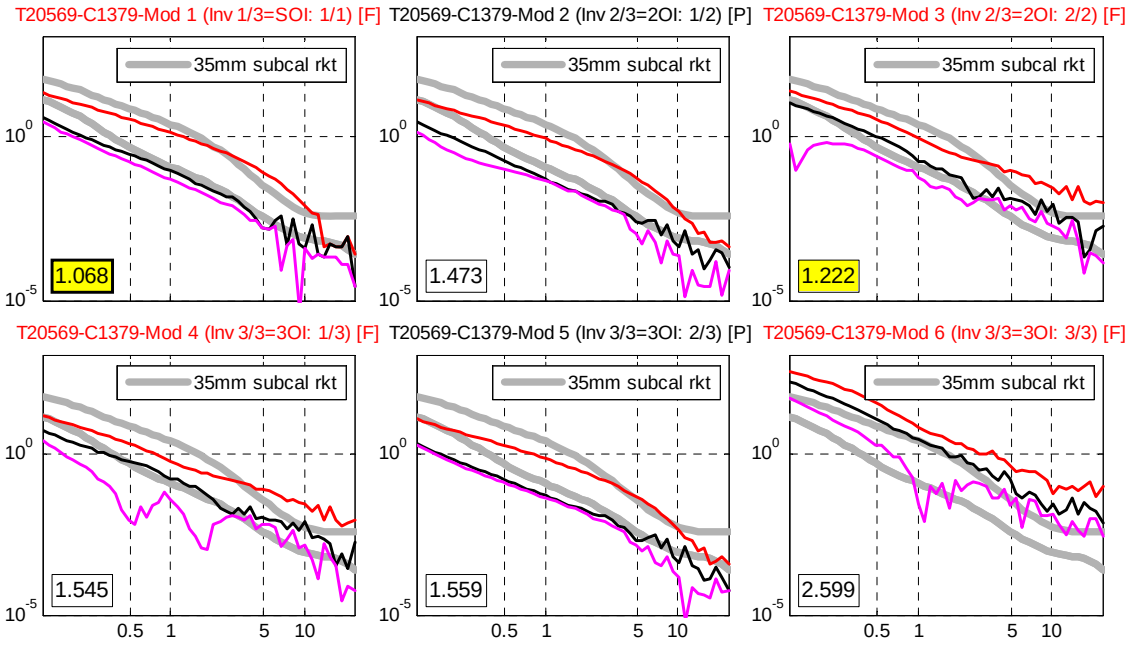

Figure 33. Polarizabilities for All Six Models of FO-20569 (missed 35mm subcaliber rocket) Plotted against Reference 35mm Polarizabilities Based on FO-20504.

Note the inconsistency of the models. Top row: models for 1- and 2-object inversions; bottom row: models for 3-object inversion. Numbers in lower left are misfit values between observed and reference polarizabilities (smaller number implies better fit).

4.2.3.3 Missed TOI: 20mm projectiles (3: FO-40546, 40655 and 40771)

The three missed 20mm projectiles are shown in Figure 34, and their polarizabilities are shown in Figure 35. In principle, these three missed TOI represent the most serious miss for a number of reasons: The polarizabilities for these items are quite consistent and therefore one or more of these items could have been found through a more thorough cluster analysis. Also, the polarizabilities are fairly consistent with 20mm reference items in our collection of reference items. In practice, due to their small size, and because a lot of small scrap has very similar polarizabilities, it is still difficult to find 20mm items without digging a huge amount of scrap. A cluster that would include the three missed TOI would likely include a lot of other items, so that, short of being lucky enough to choose one of the TOI for training out of the large cluster, the only way to assure digging all 20mm TOI would be to dig a very large amount of small scrap. We did, in fact, request training data for some 20mm-like items (FO-30345 and 20401), but both of these turned out to be small frag. Fortunately the objective for this study was to find 95% of all TOI, so that, even with the eleven missed TOI, we did achieve that goal.

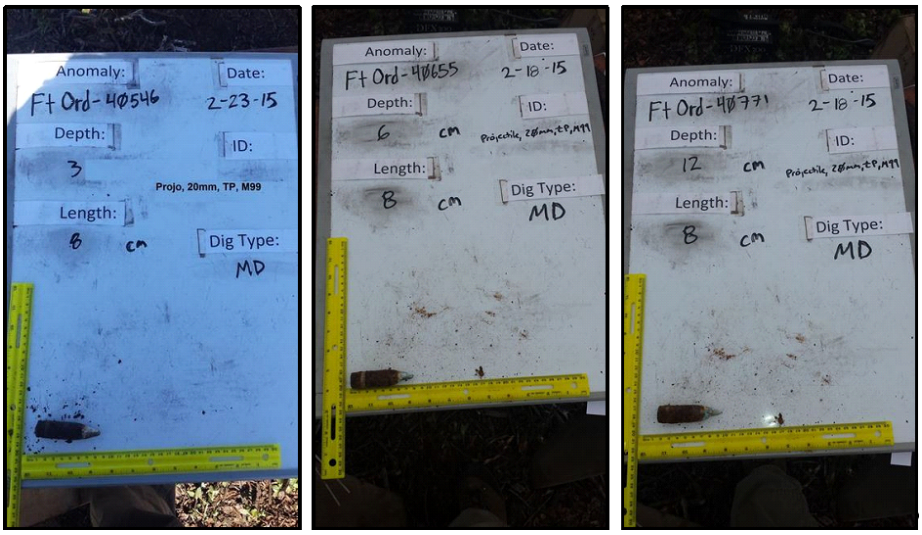

Figure 34. Three Missed 20mm Projectiles: FO-40546, 40655 and 40771.

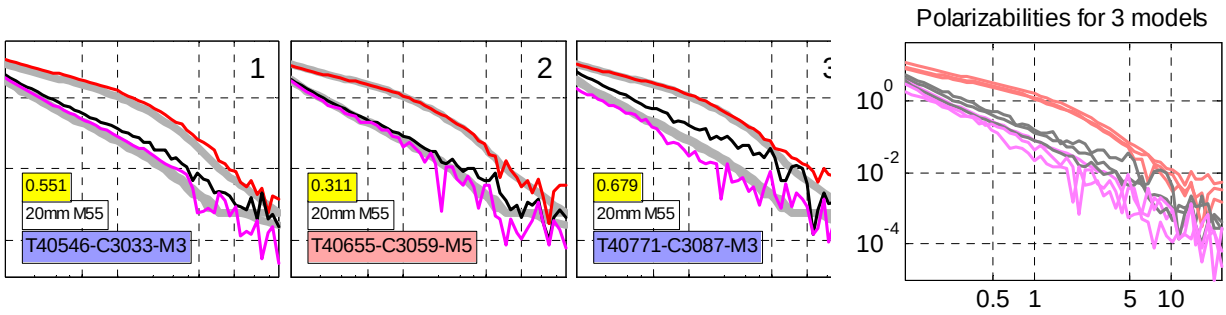

Figure 35. (1-3) Polarizabilities for the Three Missed 20mm Projectiles.

Reference polarizabilities (broken grey lines are taken from the UX-Analyze library for an M55 20mm projectiles at 10 cm depth. Numbers in yellow are misfits with respect to the reference polarizabilities. Note that for FO-4771, the misfit value was large enough so that, given our dig threshold of 0.6, this item would not have been dug even if we were looking for 20mm projectiles. Right: polarizabilities overlain to show consistency.

4.2.3.4 Missed TOI: 60mm illumination round (FO-10032)

The polarizabilities for FO-10032 are shown in Figure 36. None are a good match to Ford Ord test pit measurements of a 60mm item. Models 1, 3 and 5 are self-consistent, suggesting these are the representative response for this item. However, these polarizabilities are not a good match to any of the 33 60mm items in our large reference library.

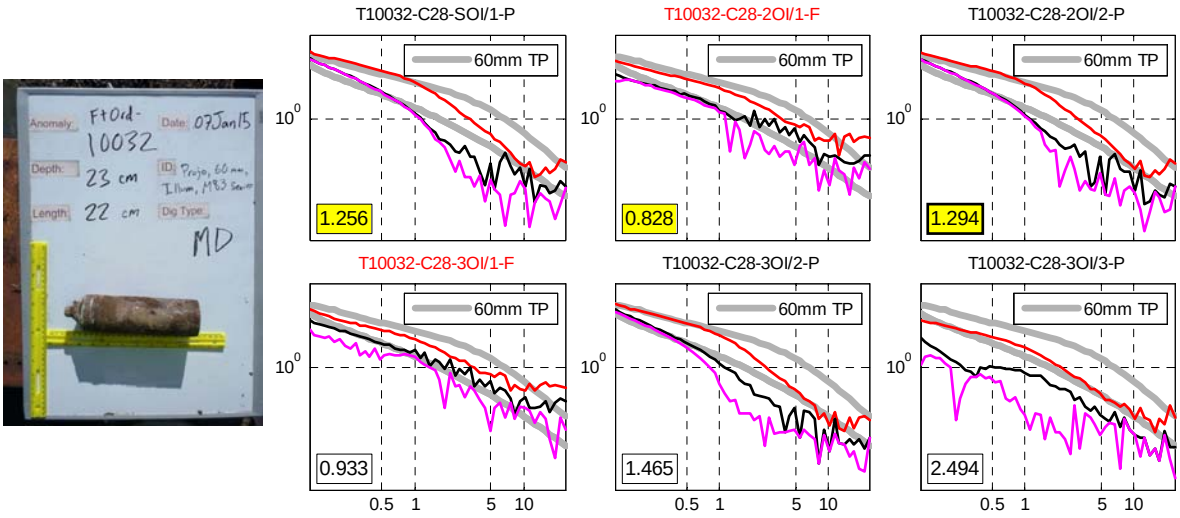

Figure 36. Left: Ground Truth Photo for Missed 60mm FO-10032. Right: Polarizabilities for All Models Plotted Against 60mm Polarizabilities Taken from Test Pit Measurements at Fort Ord (broken grey lines).

Surprisingly, two of the models (2 and 4) are actually fairly consistent with measurements of a 60mm item made at Camp Beale (Figure 37). However, the location of both of these models lies to the southeast on the horizontal inversion boundary, at a distance of 80-85 cm from the center of the sensor (which is located precisely on the target pick). Both models are actually much closer to the target location for FO-10117. This anomaly corresponds to a shallow (1 cm) 40mm projectile, so the similarity between the polarizabilities of model 2 and 4 with the Beale 60mm polarizabilities may be nothing more than coincidence. Both models 2 and 4 were failed (because of their large offset from the sensor location and apparent association with target FO-10117), and hence not used for classification. Regardless, because the Beale 60mm polarizabilities were not included in library used for classification at Fort Ord, this TOI was destined to be not dug.

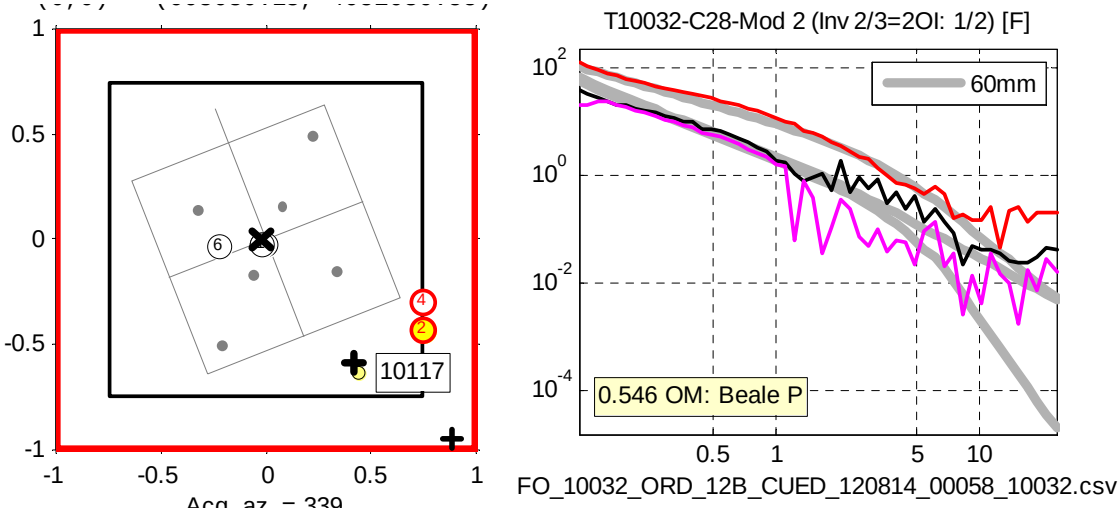

Figure 37. Left: Predicted Model Locations for FO-10032 (numbered circles). Right: Polarizabilities for Model 2.

Left: Light grey lines and dots show the MetalMapper receiver and transmitter locations. Broken black line are the horizontal inversion bounds. Models 2 and 4 lie on the inversion bounds near the target location of FO-10117. Thick "X" is the reported location of the 60mm round. Right: These are a fairly good match to a 60mm item from Camp Beale. Both model 2 and 4 were considered unreliable due to their large offset from the center of the sensor (80-85 cm) and their apparent association with FO-10117.

5.0 CONCLUSIONS AND RECOMMENDATIONS FOR FUTURE WORK

A key result of this demonstration is the reduction in false alarms that can be achieved using long off-time (25 ms) dynamic MetalMapper data. If the primary objective of detecting large TOI is pursued in future work, then the MetalMapper should be used for DGM. Although dynamic MetalMapper production rates will be significantly lower than with a conventional EM61 array, the MetalMapper's improved resolution and clutter rejection are necessary for reliable detection of large TOI at Fort Ord.

For this demonstration, the primary objective of confident classification of large munitions such as 155mm projectiles was achieved using the MetalMapper cued data acquired in low, medium and high density grids. All large TOI were identified in our classification diglist. However, two missed seed items in our stage one submission do indicate that a conservative approach is required to achieve the primary objective. In particular, we found that the data misfit threshold for identifying "can't analyze" scenarios had to be relaxed in order to ensure that all large TOI were identified.

There is a significant range of TOI at Fort Ord, and we found that some smaller items (e.g. 35 mm rockets) were difficult to distinguish from the clutter at this site. Although there were 11 small TOI missed in our cued MetalMapper diglist, the classification results indicate that 95% of smaller munitions can be confidently classified within the range of background conditions at Fort Ord.

APPENDIX A POINTS OF CONTACT

Point of Contact Name	Organization Name Address	Phone Fax Email	Role in Project
Kevin Kingdon	Black Tusk Geophysics 401-1755, W Broadway Vancouver, BC V6J 4S5, Canada	Tel: 604-428-3380 kevin.kingdon@btgeophysics.com	Project PI
Dr. Herb Nelson	ESTCP Program Office 4800 Mark Center Drive, Suite 17D03 Alexandria, VA 22350-3605	Tel: 571-372-6400 herbert.h.nelson10.civ@mail.mil	ESTCP MR Program Manager